

Supporting Information

Article title: **High resolution Mass spectrometry imaging of plant tissues: Towards a plant metabolite atlas**

Authors: Dhaka Ram Bhandari¹, Qing Wang², Wolfgang Friedt², Bernhard Spengler¹, Sven Gottwald^{2*}, Andreas Römpf^{1*}

¹Justus Liebig University Giessen, Institute of Inorganic and Analytical Chemistry,
Schubertstrasse 60, building 16, 35392 Giessen, Germany

²Justus Liebig University Giessen, Department of Plant Breeding, IFZ, Justus Liebig University
Giessen, Heinrich-Buff-Ring 26-32, 35392 Giessen, Germany

Article acceptance date: 28 Aug 2015.

The following Supporting Information is available for this article:

- Table S1.** List of metabolites imaged in oilseed rape based on accurate mass measurement.
- Notes S1.** Cyclic Spermidine conjugates, spatio-temporal metabolite distributions and hypothetical functions in developing hypocotyl and radicle
- Notes S2** Spatio-temporal distributions of sinapate esters and kaempferol glycosides
- Fig. S1.** Single pixel MS analysis of shoot apical meristem region
- Fig. S2.** Single pixel MS analysis of inner cotyledon
- Fig. S3.** Single pixel MS analysis of putative nucellar tissue
- Fig. S4.** Single pixel MS analysis of seed coat
- Fig. S5.** Single pixel MS analysis of emerging radicle
- Fig. S6.** Selected ion images of metabolites in germinating oilseed rape
- Fig. S7.** Selected ion images of metabolites in mature oilseed rape
- Fig. S8.** Scheme of metabolomic network associated with sinapate ester metabolism
- Fig. S9.** Structures corresponding to metabolite images shown in Figure S8 / Figure 2
- Fig. S10.** MS imaging of wheat seed at positive and negative ion mode
- Fig. S11.** MS imaging of rice root cross section taken from the elongation zone
- Fig. S12.** Fluorescence microscopy on cross sections of *Fusarium graminearum* infected and uninfected wheat seed
- Fig. S13.** Detection of carnitine and (trimethylammonio)but-2-enoate metabolites in wheat seed infected with *Fusarium graminearum*
- Fig. S14.** MS imaging of wheat leaf blade
- Fig. S15.** MS imaging of young oilseed rape stem
- Methods S1.** Chemicals
- Methods S2.** Generation of plant material

Table S1: List of metabolites imaged in oilseed rape based on accurate mass measurement.

Numbers in first column refer to the numbering of single MS images arranged in supporting information Fig. S1 and S2. Last column gives cited references for metabolites detected in previous studies on mature seeds of oilseed rape (typically by using LC-MS/MS methods). The reference details are provided below the table. Abbreviations: G, Guaiacyl moiety; S, syringyl moiety; UC, unknown compound.

No.	Compounds	Molecular formula	Adduct	Theoretical Mass	Mass accuracy / ppm		Reference
					Mature seed	Germinating seed	
Phenolic choline esters							
- Sinapoylcholine (SC)							
1	Sinapine (Sinapoylcholine)	C ₁₆ H ₂₃ NO ₅	[M+H] ⁺	310.16490	-0.56	-0.84	[2], [3], [6]
2	SC 4-O-glucoside	C ₂₂ H ₃₃ NO ₁₀	[M+H] ⁺	472.21772	0.53	0.51	[3], [6], [7]
3	SC(4-O-8')G 4-O'-hexoside	C ₃₂ H ₄₅ NO ₁₄	[M+H] ⁺	668.29128	-0.33	0.42	[2], [3], [6]
4	SC 4-O-dihexoside	C ₂₈ H ₄₃ NO ₁₅	[M+K] ⁺	672.22643	x	0.25	[3]
5	SC(4-O-8#)S	C ₂₇ H ₃₇ NO ₁₀	[M+H] ⁺	536.24902	1.29	1.96	[2], [3], [6]
- Sinapate choline esters							
6	Sinapic acid (Sinapate)	C ₁₁ H ₁₂ O ₅	[M+H] ⁺	225.07575	1.01	0.18	[6]
7	Sinapyl aldehyde	C ₁₁ H ₁₂ O ₄	[M+H-H ₂ O] ⁺	191.07027	0.86	-0.21	
8	Methyl sinapate	C ₁₂ H ₁₄ O ₅	[M+H-H ₂ O] ⁺	221.08084	0.58	0.23	[3]
- Feruloylcholine (FC)							
9	Feruloylcholine	C ₁₅ H ₂₁ NO ₄	[M+H] ⁺	280.15433	-0.10	-0.04	[2], [3], [6]
10	FC(4-O-8')G	C ₂₅ H ₃₃ NO ₈	[M+H] ⁺	476.22789	0.43	0.46	[2], [3], [6]
11	FC(4-O-8')G 4-O'-hexoside	C ₃₁ H ₄₃ NO ₁₃	[M+H] ⁺	638.28072	-0.04	0.13	[2], [3], [6]
12	FC(5-8#)G	C ₂₅ H ₃₁ NO ₇	[M+H] ⁺	458.21733	0.43	0.44	[2], [3], [6]
13	FC(4-O-8')S	C ₂₆ H ₃₅ NO ₉	[M+H] ⁺	506.23846	0.70	0.61	[2], [3], [6], [7]
14	5-hydroxy-FC	C ₁₅ H ₂₁ NO ₅	[M+H] ⁺	296.14925	-0.16	-0.24	[2], [3], [6]
15	FC 4-O-hexoside	C ₂₁ H ₃₁ NO ₉	[M+H] ⁺	442.20716	x	0.29	[3], [6]
- Syringoylcholine (SyC)							
16	Syringoylcholine	C ₁₄ H ₂₁ NO ₅	[M+H] ⁺	284.14925	x	-0.46	[3]
17	SyC 4-O-hexoside	C ₂₀ H ₃₁ NO ₁₀	[M+H] ⁺	446.20207	x	0.25	[2], [3], [6]
Miscellaneous phenolic choline esters							
18	Vanilloylcholine 4-O-hexoside	C ₁₉ H ₂₉ NO ₉	[M+H] ⁺	416.19151	-0.41	-0.43	[2], [3], [6]
19	Benzoylcholine	C ₁₂ H ₁₇ NO ₂	[M+H] ⁺	208.13321	1.02	0.19	[2], [3], [6]
Phenolic choline esters -							

Unknown*							
20	UC#1 (choline ester)	C ₁₈ H ₃₃ NO ₄	[M+H] ⁺	328.24823	0.08	-0.30	[3], [6]
	UC#1 (choline ester)	C ₁₈ H ₃₃ NO ₄	[M+H-H ₂ O] ⁺	310.23767		-0.84	[3], [6]
21	UC#2 (choline ester)	C ₂₅ H ₃₀ N ₂ O ₆	[M+H] ⁺	455.21766	0.08	-0.18	[3], [6]
22	UC#3 (phenolic choline ester)	C ₂₆ H ₃₅ NO ₈	[M+H] ⁺	490.24354	0.58	-0.22	[3], [6]
23	UC#6 (phenolic choline ester)	C ₃₀ H ₄₃ NO ₁₃	[M+H-H ₂ O] ⁺	608.27015		0.39	[3], [6]
24	UC#7 (phenolic choline ester)	C ₁₅ H ₂₅ NO ₄	[M+H] ⁺	284.18563		0.00	[3], [6]
25	UC#8 (phenolic choline ester)	C ₁₇ H ₂₇ NO ₄	[M+H] ⁺	310.20128		-0.81	[3], [6]
26	UC#9 (phenolic choline ester)	C ₂₆ H ₄₁ NO ₁₂	[M+H] ⁺	560.27015	-0.52	0.30	[3], [6]
Cyclic spermidine conjugate							
27	Cyclic spermidine conjugate	C ₂₇ H ₃₃ N ₃ O ₆	[M+H] ⁺	496.24421	0.43	0.42	[1], [3], [4], [6], [7]
	Cyclic spermidine conjugate	C ₂₇ H ₃₃ N ₃ O ₆	[M+Na] ⁺	518.22616	0.86	0.60	"
	Cyclic spermidine conjugate	C ₂₇ H ₃₃ N ₃ O ₆	[M+K] ⁺	534.20009	0.75	0.58	"
	Cyclic spermidine conjugate	C ₂₇ H ₃₃ N ₃ O ₆	[M+H-H ₂ O] ⁺	478.23365	0.57	0.84	"
28	N1,N5,N10-Tricaffeoyl spermidine	C ₃₄ H ₃₇ N ₃ O ₉	[M+K] ⁺	670.21614	0.50	-0.12	
	N1,N5,N10-Tricaffeoyl spermidine	C ₃₄ H ₃₇ N ₃ O ₉	[M+H] ⁺	632.26026	-0.99	0.02	
	N1,N5,N10-Tricaffeoyl spermidine	C ₃₄ H ₃₇ N ₃ O ₉	[M+Na] ⁺	654.24220	-0.18	0.17	
Phenolic compounds							
- Kaempferol glucosides							
				0.00000			
29	Sinapoly glucose	C ₁₇ H ₂₀ O ₉	[M+H] ⁺	369.11801	-0.58	-0.95	
30	Kaempferol glucoside	C ₂₁ H ₂₀ O ₁₁	[M+H] ⁺	449.10784	0.69	0.18	[1], [3], [6]
31	Kaempferol sophoroside glucoside	C ₃₃ H ₄₀ O ₂₁	[M+K] ⁺	811.16937	0.25	0.79	[1], [6]
	Kaempferol sophoroside glucoside	C ₃₃ H ₄₀ O ₂₁	[M+Na] ⁺	795.19543	0.20	-0.04	"
	Kaempferol sophoroside glucoside	C ₃₃ H ₄₀ O ₂₁	[M+H] ⁺	773.21348		0.34	"
32	Kaempferol sinapoyl sophoroside	C ₃₈ H ₄₀ O ₂₀	[M+K] ⁺	855.17445		0.55	
33	Kaempferol sinapoylsophoroside glucoside	C ₄₄ H ₅₀ O ₂₅	[M+H] ⁺	979.2714	-0.02	0.93	
- Flavones and Flavonols							
34	Laricitrin galactoside	C ₂₂ H ₂₂ O ₁₃	[M+Na] ⁺	517.09526	0.85	0.99	
35	Laricitrin triglucoside	C ₃₄ H ₄₂ O ₂₃	[M+Na] ⁺	841.20091	0.58	0.64	
36	Tetra methoxy methylenedioxy flavone	C ₂₀ H ₁₈ O ₈	[M+H] ⁺	387.10744	-0.53	-0.93	
37	Trihydroxy trimethoxy flavone isovalerate	C ₂₃ H ₂₄ O ₉	[M+NH ₄] ⁺	462.17586	0.42	0.32	
- Flavanone							
38	Naringenin coumaroylglucoside	C ₃₀ H ₂₈ O ₁₂	[M+NH ₄] ⁺	598.19190	0.48	0.40	
39	Tetrahydroxy methoxyflavanone	C ₁₆ H ₁₄ O ₇	[M+H] ⁺	319.08123	0.60	0.16	
- Flavans, Flavanols and Leucoanthocyanidins							
40	Epicatechin cinnamoyl	C ₃₀ H ₃₀ O ₁₂	[M+NH ₄] ⁺	600.20755	0.36	0.23	

	allopyranoside					
41	Epigui bourtinidolalpaol	C ₁₅ H ₁₄ O ₅	[M+H] ⁺	275.09140	0.32	-0.47
	- Anthocyanidins					
42	Cyanidin caffeylrutinoside	C ₃₆ H ₃₇ O ₁₈	[M+H] ⁺	758.20527	0.43	0.55
43	Malvidin rutinoside	C ₂₉ H ₃₅ O ₁₆	[M+H-H ₂ O] ⁺	622.18922	0.42	0.64
	Malvidin rutinoside	C ₂₉ H ₃₅ O ₁₆	[M+Na] ⁺	662.18173	0.77	0.60
44	Cyanidin sophorotrioside	C ₃₃ H ₄₁ O ₂₁	[M+H] ⁺	774.22131		0.00
	Miscellaneous phenolic compounds					
45	Coumaric acid	C ₉ H ₈ O ₃	[M+H] ⁺	165.05462	1.09	0.79
46	Trimethoxycoumarin	C ₁₂ H ₁₂ O ₅	[M+H] ⁺	237.07575	0.09	-0.13
47	Caffeic Acid	C ₉ H ₈ O ₄	[M+H] ⁺	181.04954	0.79	0.22
48	Vinyl caffate	C ₁₁ H ₁₀ O ₄	[M+H] ⁺	207.06519	0.70	0.29
49	Caffeyl alcohol	C ₉ H ₁₀ O ₃	[M+H] ⁺	167.07027	1.03	0.54
50	Butyl caffeyolquinat	C ₂₀ H ₂₆ O ₉	[M+NH ₄] ⁺	428.19151	0.32	0.23
51	Phenylpropioic acid	C ₉ H ₆ O ₂	[M+NH ₄] ⁺	164.07060	0.72	0.37
52	Methyl trimethoxycinnamate	C ₁₃ H ₁₆ O ₅	[M+H] ⁺	253.10705	0.05	-0.20
53	Benzoic acid	C ₁₃ H ₁₄ O ₈	[M+H] ⁺	299.07614	-0.76	-0.57
	Lipids					
	- Phosphatidylcholines (PC)					
54	PC(34:2)	C ₄₂ H ₈₀ NO ₈ P	[M+K] ⁺	796.52531	0.89	1.17
55	PC(34:3)	C ₄₂ H ₇₈ NO ₈ P	[M+K] ⁺	794.50966	0.56	0.78
	PC(34:3)	C ₄₂ H ₇₈ NO ₈ P	[M+H] ⁺	756.55378	0.17	0.67
56	PC(36:5)	C ₄₄ H ₇₈ NO ₈ P	[M+K] ⁺	818.50966	0.60	0.87
	PC(36:5)	C ₄₄ H ₇₈ NO ₈ P	[M+H] ⁺	780.55378	-0.13	-1.09
	PC(36:5)	C ₄₄ H ₇₈ NO ₈ P	[M+Na] ⁺	802.53573	0.83	0.47
57	PC(38:3)	C ₄₆ H ₈₆ NO ₈ P	[M+K] ⁺	850.57226	0.59	1.02
	PC(38:3)	C ₄₆ H ₈₆ NO ₈ P	[M+H] ⁺	812.61638	0.54	-0.23
	PC(38:3)	C ₄₆ H ₈₆ NO ₈ P	[M+Na] ⁺	834.59833		0.06
58	PC(36:4)	C ₄₄ H ₈₀ NO ₈ P	[M+H] ⁺	782.56943	0.32	1.20
	PC(36:4)	C ₄₄ H ₈₀ NO ₈ P	[M+Na] ⁺	804.55138	0.61	0.72
	PC(36:4)	C ₄₄ H ₈₀ NO ₈ P	[M+K] ⁺	820.52531	1.02	1.12
59	PC(36:3)	C ₄₄ H ₈₂ NO ₈ P	[M+H] ⁺	784.58508	0.84	1.10
60	LysoPC(18:2)	C ₂₆ H ₅₀ NO ₇ P	[M+K] ⁺	558.29565	0.57	0.48
	LysoPC(18:2)	C ₂₆ H ₅₀ NO ₇ P	[M+Na] ⁺	542.32171	0.34	0.77
	LysoPC(18:2)	C ₂₆ H ₅₀ NO ₇ P	[M+H] ⁺	520.33977	0.41	0.46
61	PC(40:3)	C ₄₈ H ₉₀ NO ₈ P	[M+H] ⁺	840.64768	-0.12	-0.69
62	PC(34:1)	C ₄₂ H ₈₂ NO ₈ P	[M+H] ⁺	760.58508	0.42	1.14
63	LysoPC(18:1)	C ₂₆ H ₅₂ NO ₇ P	[M+H] ⁺	522.35542	0.44	1.03
	LysoPC(18:1)	C ₂₆ H ₅₂ NO ₇ P	[M+Na] ⁺	544.33736	0.82	1.40
	LysoPC(18:1)	C ₂₆ H ₅₂ NO ₇ P	[M+K] ⁺	560.31113	0.58	0.34
	- Phosphatidylglycerols (PG)					

64	PG(38:2)	C ₄₄ H ₈₃ O ₁₀ P	[M+Na] ⁺	825.56161	-0.15	1.48
-Diacylglycerols (DG)						
65	DG(34:2)	C ₃₇ H ₆₈ O ₅	[M+H-H ₂ O] ⁺	575.50339	0.43	0.45
66	DG(34:3)	C ₃₇ H ₆₆ O ₅	[M+H-H ₂ O] ⁺	573.48774	0.74	0.45
67	DG(36:2)	C ₃₉ H ₇₂ O ₅	[M+H-H ₂ O] ⁺	603.53469	1.10	1.26
68	DG(36:4)	C ₃₉ H ₆₈ O ₅	[M+H-H ₂ O] ⁺	599.50339	0.52	0.67
69	DG(38:2)	C ₄₁ H ₇₆ O ₅	[M+H-H ₂ O] ⁺	631.56599	0.63	1.35
70	DG(38:4)	C ₄₁ H ₇₂ O ₅	[M+H-H ₂ O] ⁺	627.53469	0.50	0.19
71	DG(40:2)	C ₄₃ H ₈₀ O ₅	[M+H-H ₂ O] ⁺	659.59729	0.72	1.52
72	DG(40:3)	C ₄₃ H ₇₈ O ₅	[M+H-H ₂ O] ⁺	657.58164	0.72	0.94
73	DG(42:2)	C ₄₅ H ₈₄ O ₅	[M+H-H ₂ O] ⁺	687.62859	0.19	0.38
74	DG(40:4)	C ₄₃ H ₇₆ O ₅	[M+H-H ₂ O] ⁺	655.56599	0.16	0.14
-Triacylglycerols (TG)						
75	TG(54:3)	C ₅₇ H ₁₀₄ O ₆	[M+Na] ⁺	907.77251	-0.62	-0.77
76	TG(52:4)	C ₅₅ H ₉₈ O ₆	[M+Na] ⁺	877.72556	-0.13	0.21
	TG(52:4)	C ₅₅ H ₉₈ O ₆	[M+K] ⁺	893.6995	-0.15	-0.27
77	TG(54:4)	C ₅₇ H ₁₀₂ O ₆	[M+Na] ⁺	905.75686	-0.33	-0.19
78	TG(54:5)	C ₅₇ H ₁₀₀ O ₆	[M+Na] ⁺	903.74121	0.40	0.31
	TG(54:5)	C ₅₇ H ₁₀₀ O ₆	[M+K] ⁺	919.71515	-0.20	0.13
79	TG(54:6)	C ₅₇ H ₉₈ O ₆	[M+Na] ⁺	901.72556	0.37	0.58
	TG(54:6)	C ₅₇ H ₉₈ O ₆	[M+K] ⁺	917.6995	-0.04	0.38
80	TG(54:7)	C ₅₇ H ₉₆ O ₆	[M+Na] ⁺	899.70991	0.27	0.50
81	TG(56:3)	C ₅₉ H ₁₀₈ O ₆	[M+Na] ⁺	935.80381	-0.14	0.11
	TG(56:3)	C ₅₉ H ₁₀₈ O ₆	[M+K] ⁺	951.77775	-0.01	0.71
82	TG(56:4)	C ₅₉ H ₁₀₆ O ₆	[M+Na] ⁺	933.78816	0.35	0.21
	TG(56:4)	C ₅₉ H ₁₀₆ O ₆	[M+K] ⁺	949.7621	-0.68	-0.11
83	TG(56:5)	C ₅₉ H ₁₀₄ O ₆	[M+Na] ⁺	931.77251	0.63	0.40
	TG(56:5)	C ₅₉ H ₁₀₄ O ₆	[M+K] ⁺	947.74645	-0.47	0.07
84	TG(58:4)	C ₆₁ H ₁₁₀ O ₆	[M+Na] ⁺	961.81946	-0.28	-0.08
	TG(58:4)	C ₆₁ H ₁₁₀ O ₆	[M+K] ⁺	977.7934	-0.43	0.45
85	TG(58:5)	C ₆₁ H ₁₀₈ O ₆	[M+K] ⁺	975.77775	0.23	0.41
	TG(58:5)	C ₆₁ H ₁₀₈ O ₆	[M+Na] ⁺	959.80381	-0.16	0.39
86	TG(60:4)	C ₆₃ H ₁₁₄ O ₆	[M+Na] ⁺	989.85076	-0.13	0.13
87	TG(60:5)	C ₆₃ H ₁₁₂ O ₆	[M+Na] ⁺	987.83511	0.50	0.60
88	TG(56:6)	C ₅₉ H ₁₀₂ O ₆	[M+K] ⁺	945.7308	-0.54	-0.23
89	TG(58:7)	C ₆₁ H ₁₀₄ O ₆	[M+K] ⁺	971.74645	-0.31	0.13
	TG(58:7)	C ₆₁ H ₁₀₄ O ₆	[M+Na] ⁺	955.77251	0.42	-0.39
Amino acid						
90	Arginine	C ₆ H ₁₄ N ₄ O ₂	[M+H] ⁺	175.11895	1.03	0.7
Carbohydrate						
91	Dihexose	C ₁₂ H ₂₂ O ₁₁	[M+K] ⁺	381.07937	-0.8	-1.06

92	Trihexose	$C_{18}H_{32}O_{16}$	$[M+K]^+$	543.13219	0.05	0.53
93	Tetrahexoses	$C_{61}H_{104}O_6$	$[M+K]^+$	705.18502	0.08	0.09

- [1] A. Baumert, C. Milkowski, J. Schmidt, M. Nimtz, V. Wray and D. Strack, *Phytochemistry*, 2005, **66**, 1334-1345.
- [2] C. Böttcher, E. von Roepenack-Lahaye, J. Schmidt, S. Clemens and D. Scheel, *Journal of mass spectrometry : JMS*, 2009, **44**, 466-476.
- [3] K. Clauß, E. von Roepenack-Lahaye, C. Böttcher, M. R. Roth, R. Welti, A. Erban, J. Kopka, D. Scheel, C. Milkowski and D. Strack, *Plant Physiol*, 2011, **155**, 1127-1145.
- [4] J. Fang, M. Reichelt, W. Hidalgo, S. Agnolet and B. Schneider, *PloS one*, 2012, **7**, e48006.
- [5] G. Marton, V. Pleşu, A. Marton and M. T. Bercau, 2010, **21**, 1351-1356.
- [6] J. Mittasch, C. Böttcher, A. Frolov, D. Strack and C. Milkowski, *Plant physiology*, 2013, **161**, 1656-1669.
- [7] K. Wolfram, J. Schmidt, V. Wray, C. Milkowski, W. Schliemann and D. Strack, *Phytochemistry*, 2010, **71**, 1076-1084.

Notes S1: Cyclic Spermidine conjugates, spatio-temporal metabolite distributions and hypothetical functions in developing hypocotyl and radicle

Two polyamine (PA) conjugates were detected by MS imaging (compounds 27 and 28 in Table S1). The cyclic spermidine conjugate is well known from mature seeds of oilseed rape¹⁻³ while here we also report the PA conjugate N1,N5,N10-tricaffeoyl spermidine. Cyclic spermidine conjugate has been spatially localized in the mature oilseed rape, in hypocotyl-radicle region^{1,2}. MS imaging could confirm this assignment (Fig. 1c, red), and also we could image one more conjugate (Fig. S2.28). With the beginning of germination cyclic spermidine conjugates were located in the parenchyma of hypocotyl-radicle, in the apical shoot meristem and in the radicle tip region (Fig. 1d, red), while N1,N5,N10-tricaffeoyl spermidine were limited to the parenchyma layer of emerging radicle (Fig. S1.28). Generally, PAs and PA conjugates are supposed to be implicated in several physiological processes such as cell division, flowering and responses to abiotic/biotic stresses⁴⁻⁶. However, their specific sites of activity and functional roles are still largely unknown⁷. In fact, some PA conjugates are assumed to play roles in cell division processes during the early stages of germination by supplying free PAs (e.g. spermidine) to developing tissues⁷. Against this background, it is informative that both imaged PA conjugates were exclusively mapped to parenchyma and meristem cells, which consist of rapidly dividing cells. Moreover, in germinating *Arabidopsis* the *SDT* gene, required for the degradation of PA conjugates into disinapoyl spermidine, was mainly expressed in the root tip and, in decreasing order, also in the basal region of the hypocotyl and in the cotyledons. Particularly, the *SDT* expression in the root tip has been discussed as a central supply function of spermidine to these rapidly dividing cells⁷. Therefore, it is possible to assume that both PA conjugates located by MS imaging have similar functions in cell division processes in the developing hypocotyl and/or radicle. Especially, the cyclic polyamine conjugate might be of high relevance since it has been detected in several metabolome studies on oilseed rape.

Notes S2: Spatio-temporal distributions of sinapate esters and kaempferol glycosides

For the economic value of oilseed rape, both the oil ⁸ and the sinapate ester metabolism are of great scientific interest. Sinapate negatively affect the seed meal which as high protein feed is an important by-product of oil production ⁹. However, despite their economic importance, the biological functions and topology of lipids and sinapate esters are barely known due to the lack of appropriate analytical methods for spatial mapping. During early seed development, sinapate is conjugated with choline to sinapine. The observed widespread presence of sinapine (Fig. 2) is in accordance with its assumed function as supplier of sinapate and choline for developing seedlings ¹⁰. Clauss et al., reported that a portion of sinapine accumulates in various glycosylated derivatives such as 4-O-glucoside, 4-O-di-hexoside, typically attended by sinapine esters such as feruloylcholine (Fig. 2) ¹. MS imaging demonstrated low-level accumulations of sinapate in the endosperm and hypocotyl-radicle body (Fig. 2). Sinapate are short intermediates in lignin biosynthesis ¹¹ and syringoylcholine conjugates; or into precursors for phenolics such as kaempferol glycosides ¹. For kaempferol glycosides studies confirmed their occurrence in mature oilseed rape ¹ and localization to the cotyledons ². With the help of high resolution MS imaging three kaempferol derivatives, kaempferol glycoside, kaempferol-sophoroside glucoside, and kaempferol sinapoylsophoroside glucoside could be localized to a thin layer between the cotyledons, which corresponds to adaxial (upper) cotyledon epidermis (Fig. 2). The kaempferol sinapoyl sophoroside, however, was only detected in the germinating seed. Since the upper epidermis represents the protective coat of emerging cotyledons, MS imaging could provide further evidence for the assumed role of kaempferol conjugates in protecting chlorophyll and other light-sensitive components from UV-B irradiation ¹².

References for Notes 1-2:

1. K. Clauß, E. von Roepenack-Lahaye, C. Bottcher, M. R. Roth, R. Welti, A. Erban, J. Kopka, D. Scheel, C. Milkowski and D. Strack, *Plant Physiology*, 2011, **155**, 1127-1145.
2. J. Fang, M. Reichelt, W. Hidalgo, S. Agnolet and B. Schneider, *PloS one*, 2012, **7**, e48006.
3. A. Baumert, C. Milkowski, J. Schmidt, M. Nimtz, V. Wray and D. Strack, *Phytochemistry*, 2005, **66**, 1334-1345.
4. P. J. Facchini, J. Hagel and K. G. Zulak, *Canadian Journal of Botany*, 2002, **80**, 577-589.
5. H. Kaur, N. Heinzl, M. Schottner, I. T. Baldwin and I. Galis, *Plant Physiol*, 2010, **152**, 1731-1747.
6. S. S. Gill and N. Tuteja, *Plant Signal Behav*, 2010, **5**, 26-33.

7. J. Luo, C. Fuell, A. Parr, L. Hill, P. Bailey, K. Elliott, S. A. Fairhurst, C. Martin and A. J. Michael, 2009, **21**, 318-333.
8. A. Abbadi and G. Leckband, *European Journal of Lipid Science and Technology*, 2011, **113**, 1198-1206.
9. A. Hüsken, A. Baumert, D. Strack, H. C. Becker, C. Möllers and C. Milkowski, *Molecular Breeding*, 2005, **16**, 127-138.
10. C. Milkowski and D. Strack, *Planta*, 2010, **232**, 19-35.
11. C. M. Fraser and C. Chapple, *The Arabidopsis book / American Society of Plant Biologists*, 2011, **9**, e0152.
12. D. Meißner, A. Albert, C. Böttcher, D. Strack and C. Milkowski, *Planta*, 2008, **228**, 663-674.

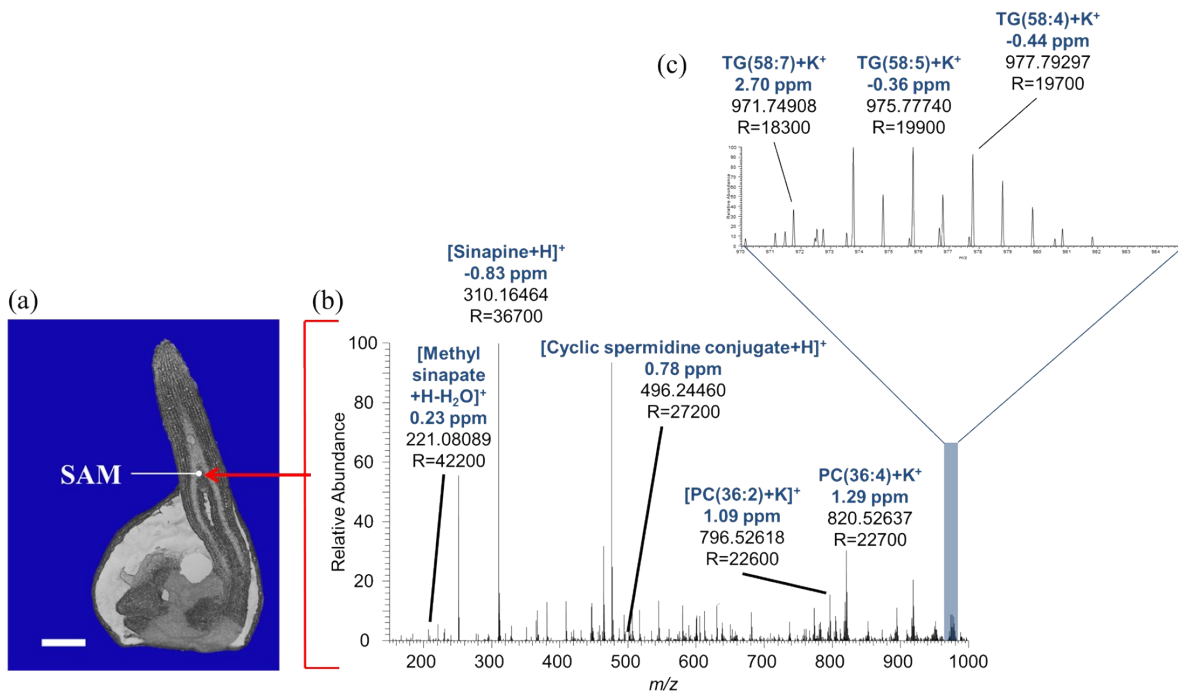


Fig. S1. Single-pixel MS analysis of shoot apical meristem region. (a) Optical image of longitudinal seed section prepared from germinating oilseed rape. The shoot apical meristem region (SAM) is indicated by white line. The red arrow marks the location of analysed single pixel. Scale bar 500 μm . (b) Single-pixel mass spectrum in a 10 μm step size measurement. (c) Zoomed in mass spectrum in the region of m/z 970-985.

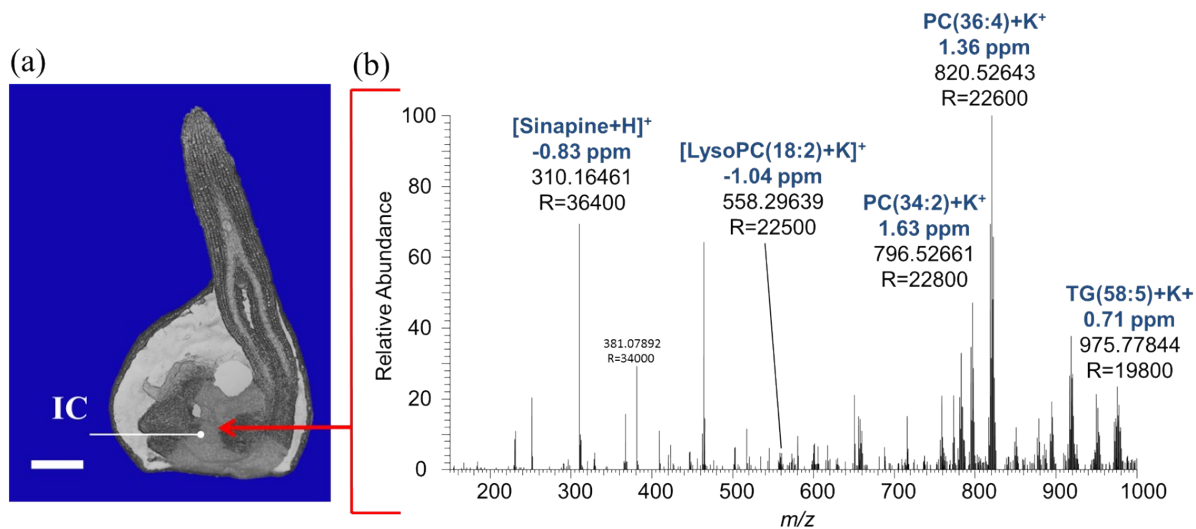


Fig. S2. Single-pixel MS analysis of inner cotyledon. (a) Optical image of longitudinal seed section prepared from germinating oilseed rape. The inner cotyledon (IC) is indicated by white line. The red arrow marks the location of analysed single pixel. Scale bar 500 μm . (b) Single-pixel mass spectrum in a 10 μm step size measurement.

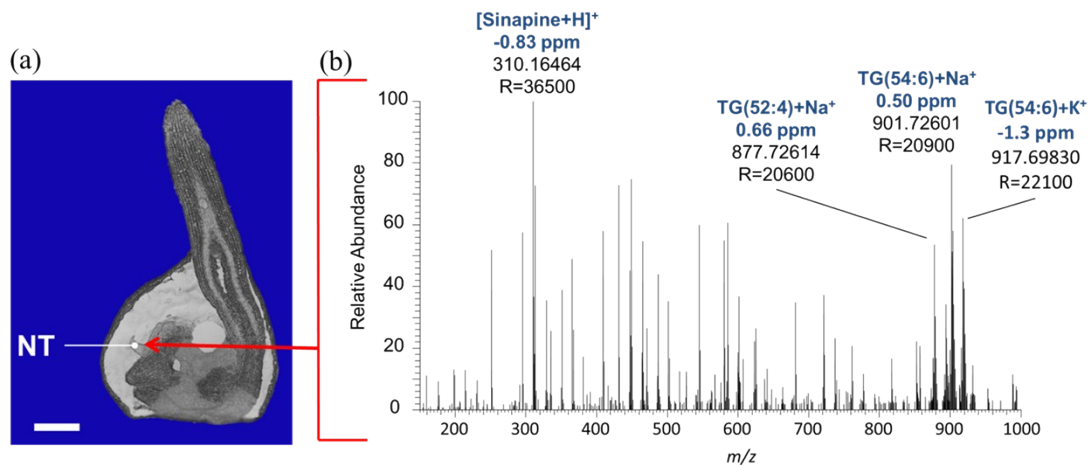


Fig. S3. Single-pixel MS analysis of putative nucellar tissue. (a) Optical image of longitudinal seed section prepared from germinating oilseed rape. The putative nucellar tissue (NT) is indicated by white line. The red arrow marks the location of analysed single pixel. Scale bar 500 μm . (b) Single-pixel mass spectrum in a 10 μm step size measurement.

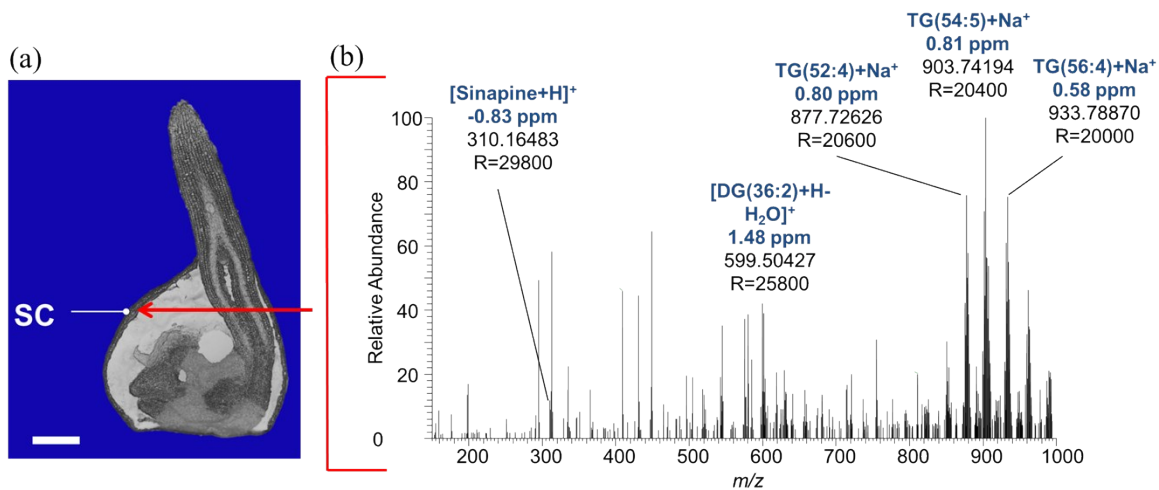


Fig. S4. Single-pixel MS analysis of seed coat. (a) Optical image of longitudinal seed section prepared from germinating oilseed rape. The seed coat (SC) is indicated by white line. The red arrow marks the location of analysed single pixel. Scale bar 500 μm. (b) Single-pixel mass spectrum in a 10 μm step size measurement.

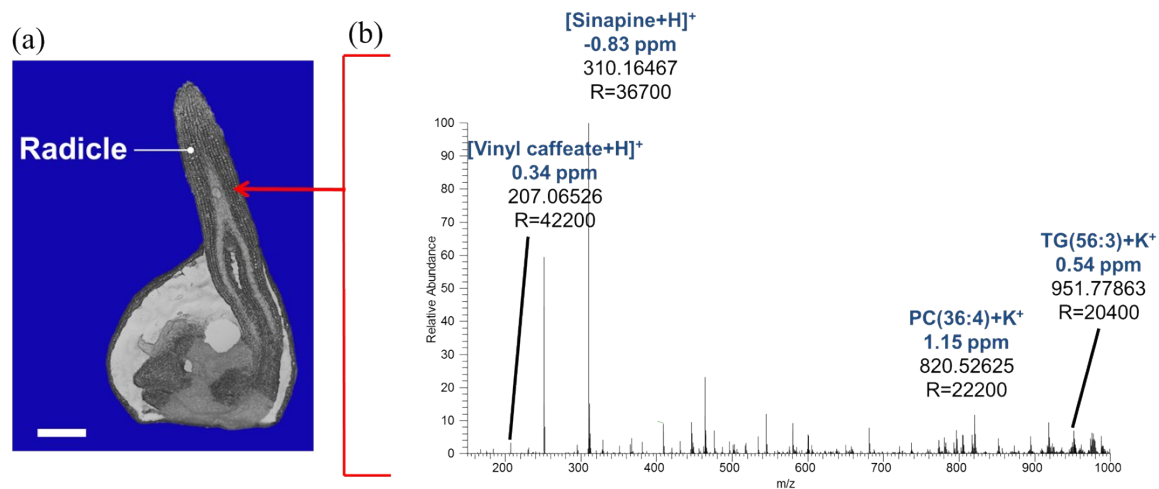


Fig. S5. Single-pixel MS analysis of emerging radicle. (a) Optical image of longitudinal seed section prepared from germinating oilseed rape. The emerging radicle (R) is indicated by white line. The red arrow marks the location of analysed single pixel. Scale bar 500 μm , (b) Single-pixel mass spectrum in a 10 μm step size measurement.

Fig. S6. Selected ion images of metabolites detected in germinating oilseed rape

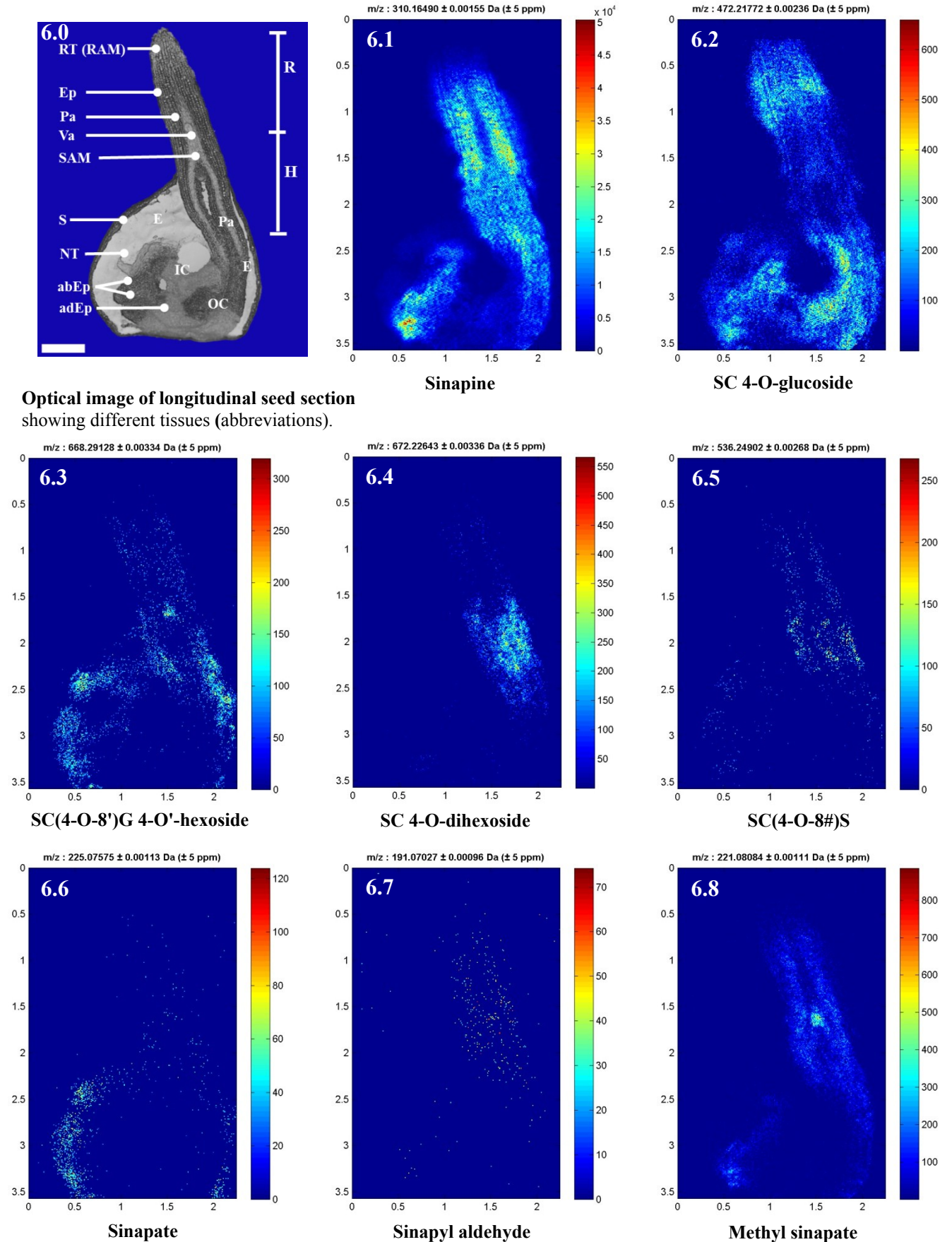


Fig. S6: continuation sheet

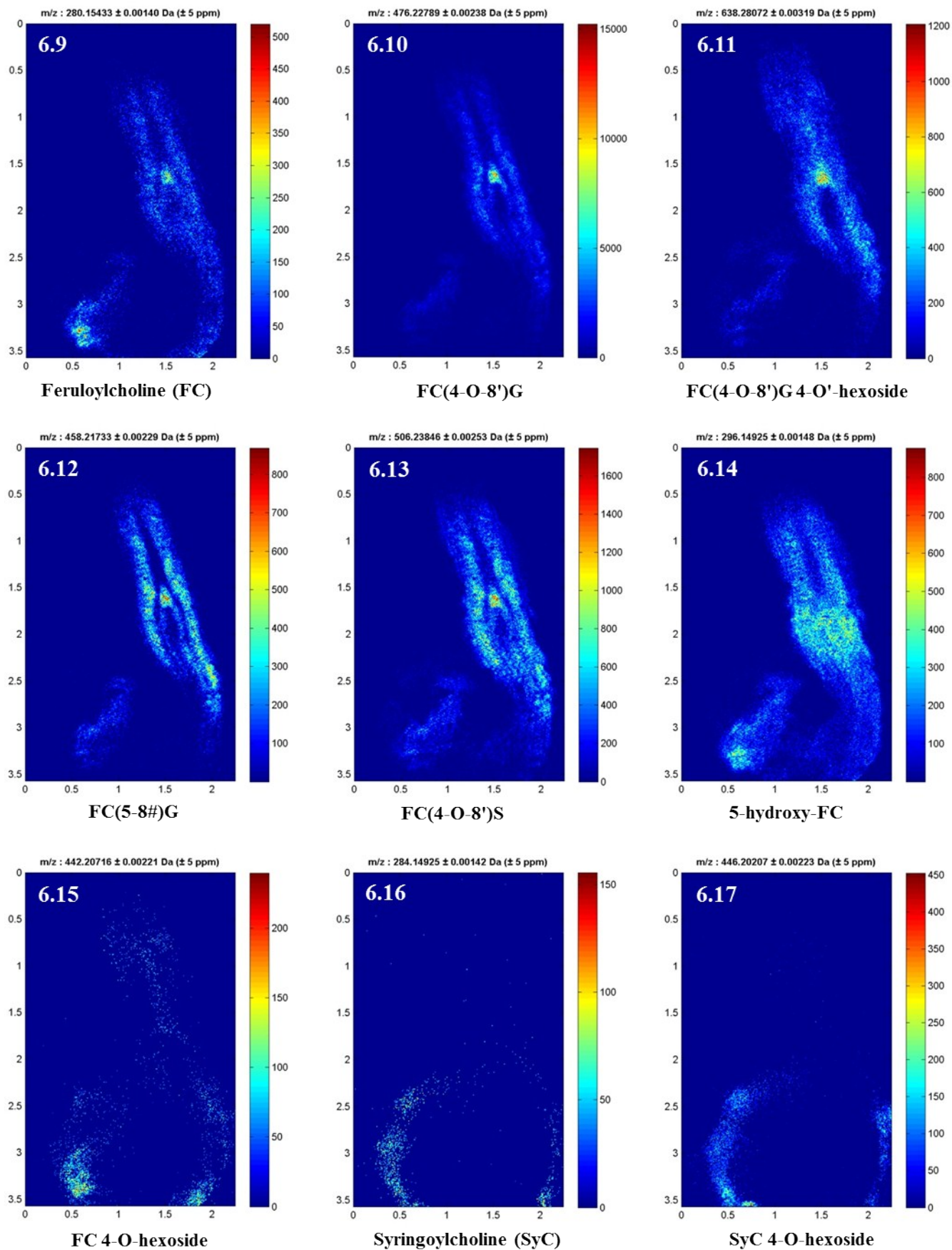


Fig. S6: continuation sheet

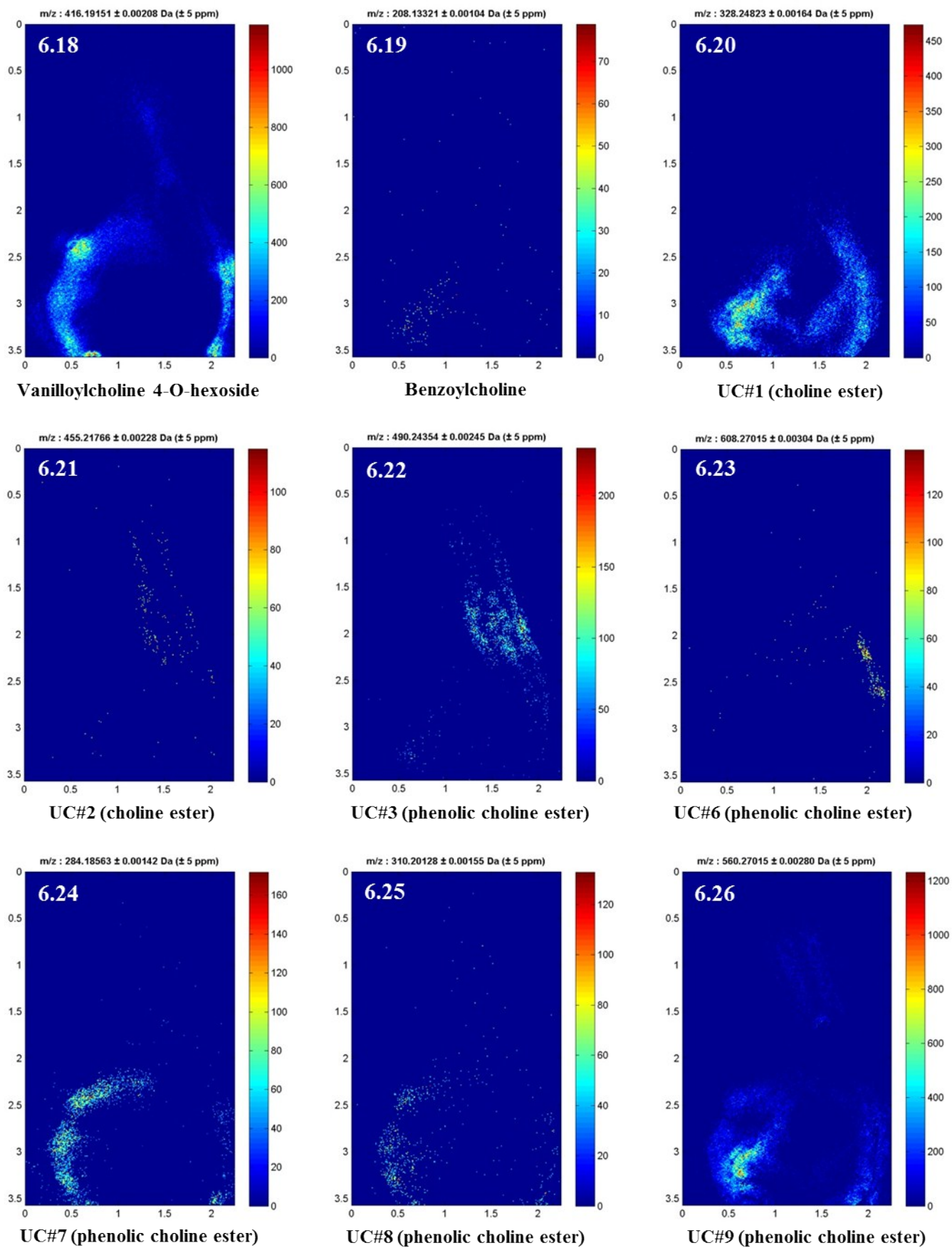


Fig. S6: continuation sheet

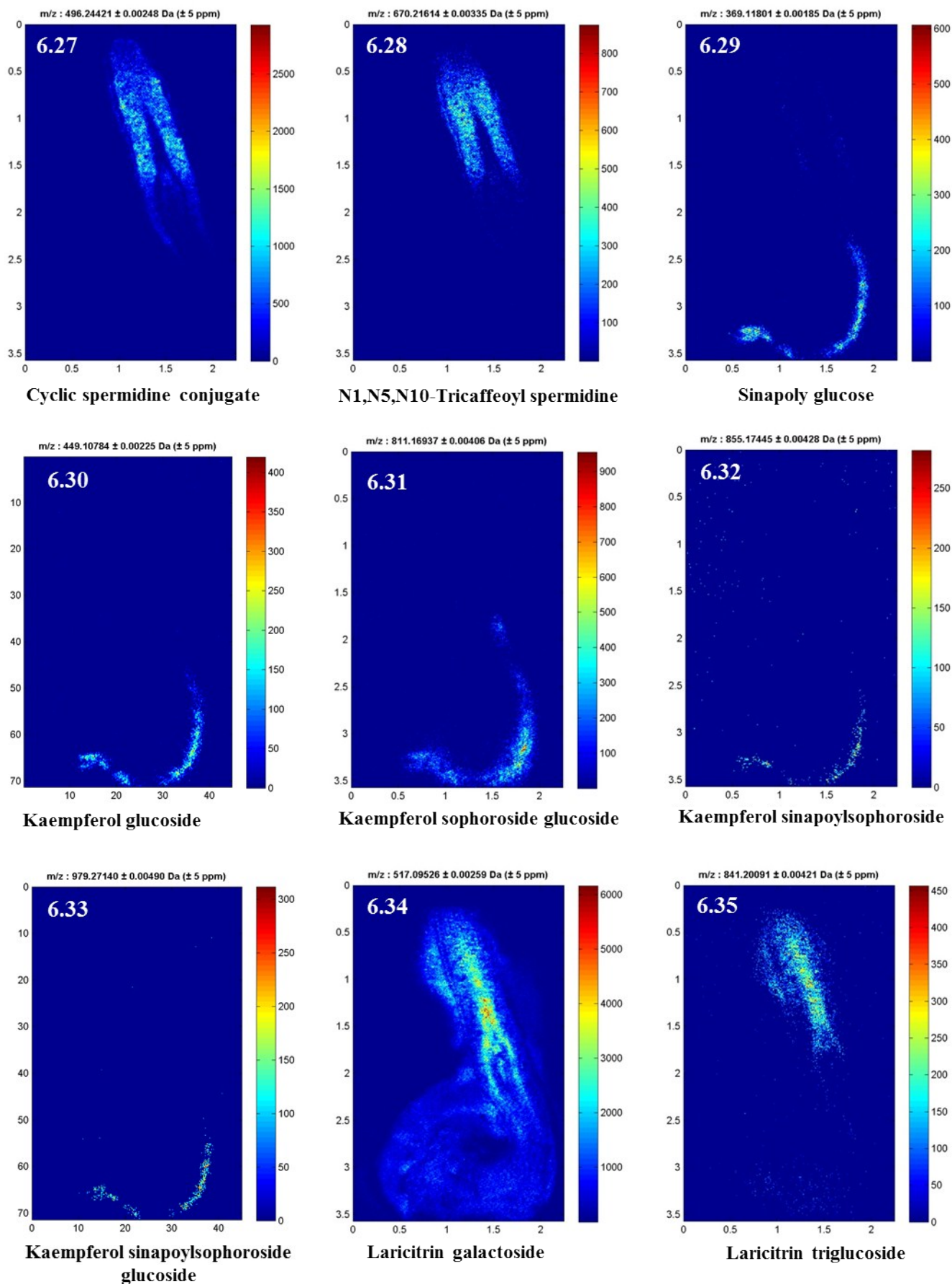
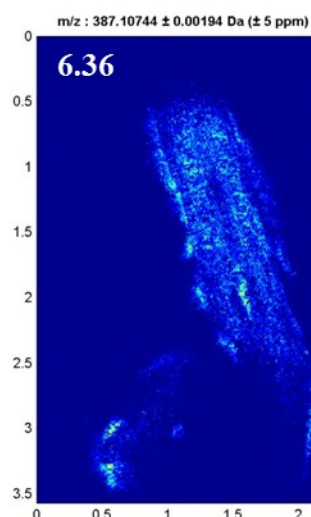
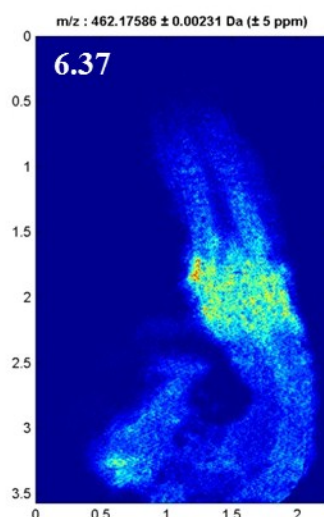


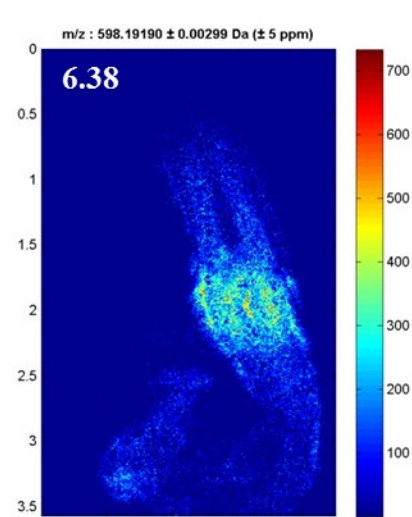
Fig. S6: continuation sheet



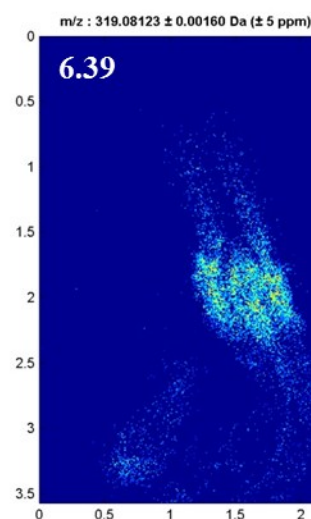
Tetra methoxy methylenedioxy flavone



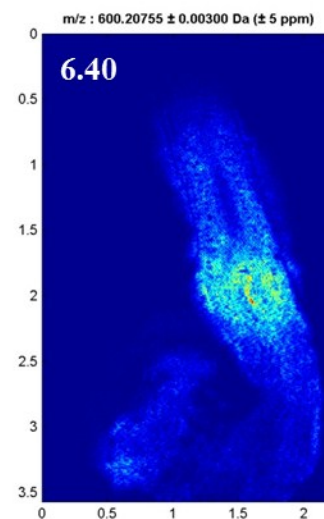
**Trihydroxy-trimethoxy-flavone -
isovalerate**



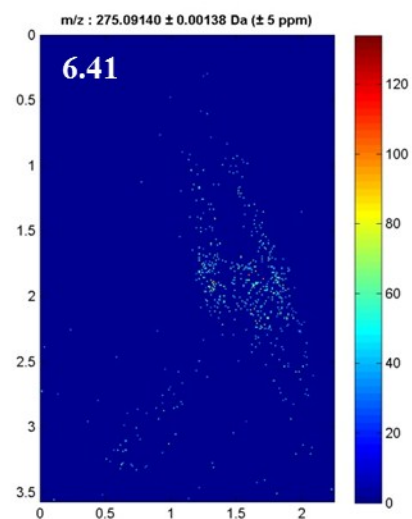
Naringenin -coumaroyl-glucoside



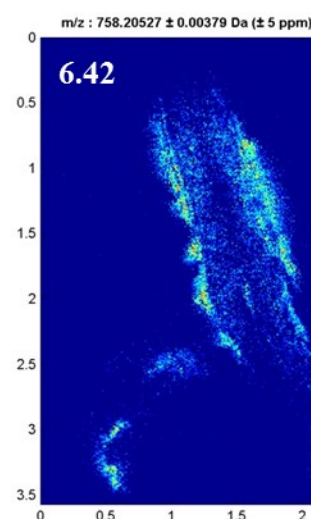
Tetrahydroxy-methoxyflavanone



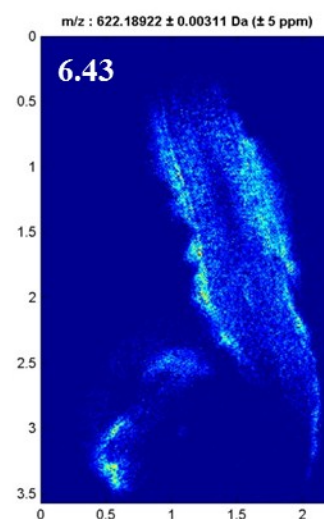
Epicatechin -cinnamoyl-allopyranoside



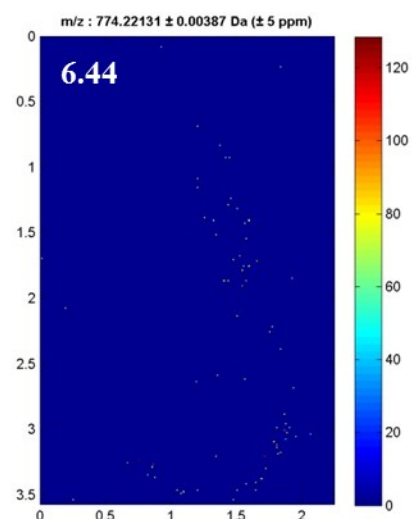
Epiguibourtinidolalpaol



Cyanidin caffeylrutinoside



Malvidin rutinoside



Cyanidin sophorotrioside

Fig. S6: continuation sheet

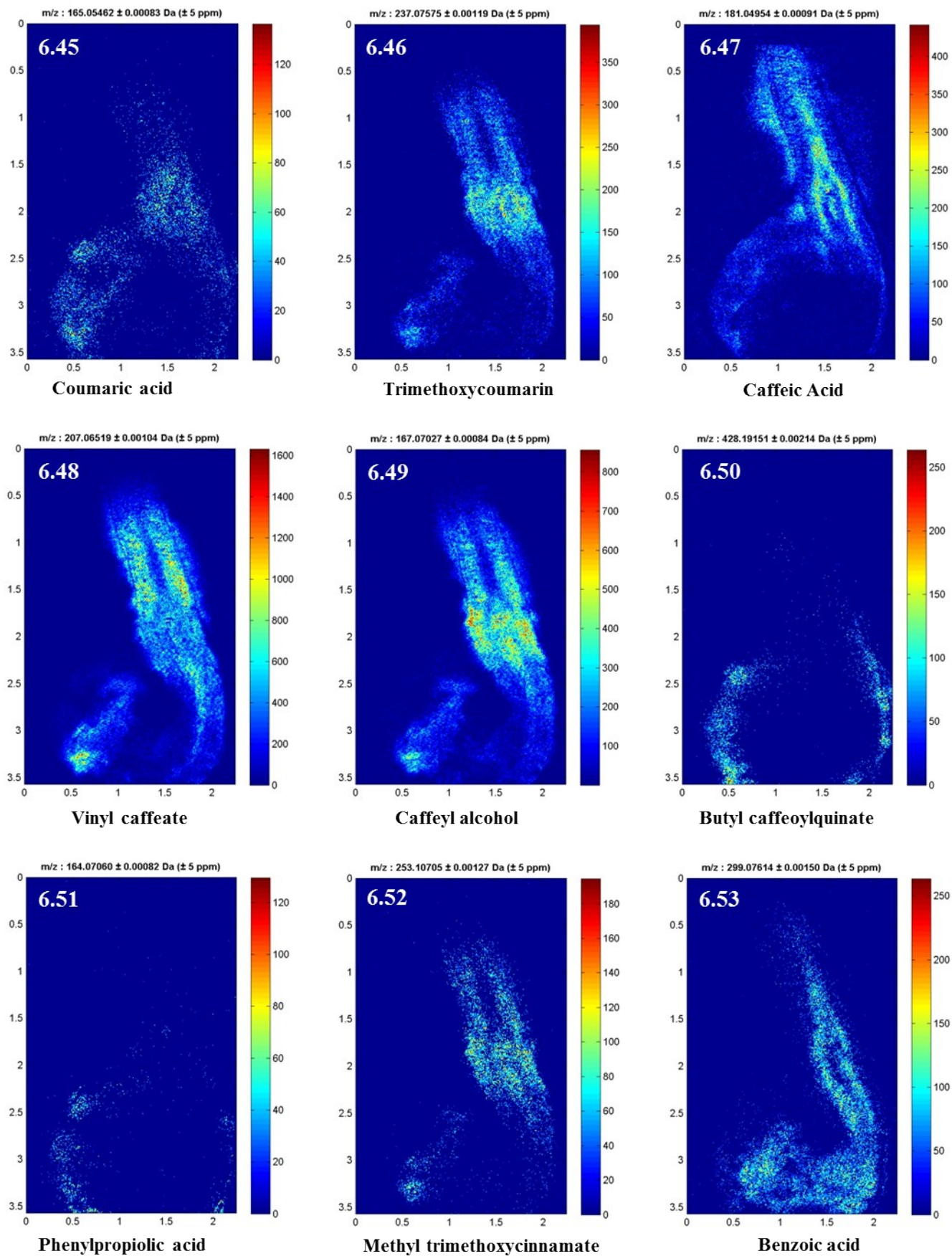


Fig. S6: continuation sheet

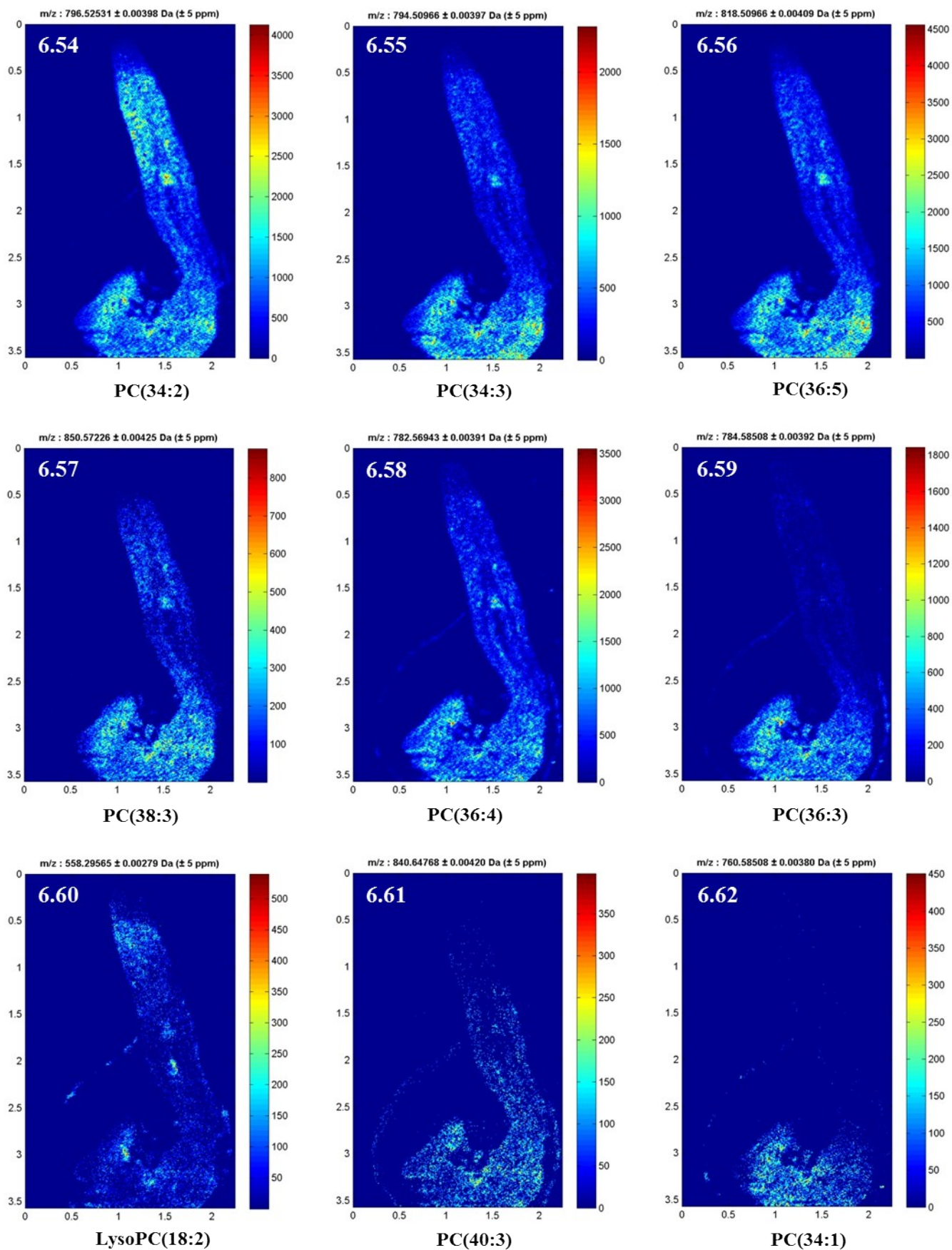


Fig. S6: continuation sheet

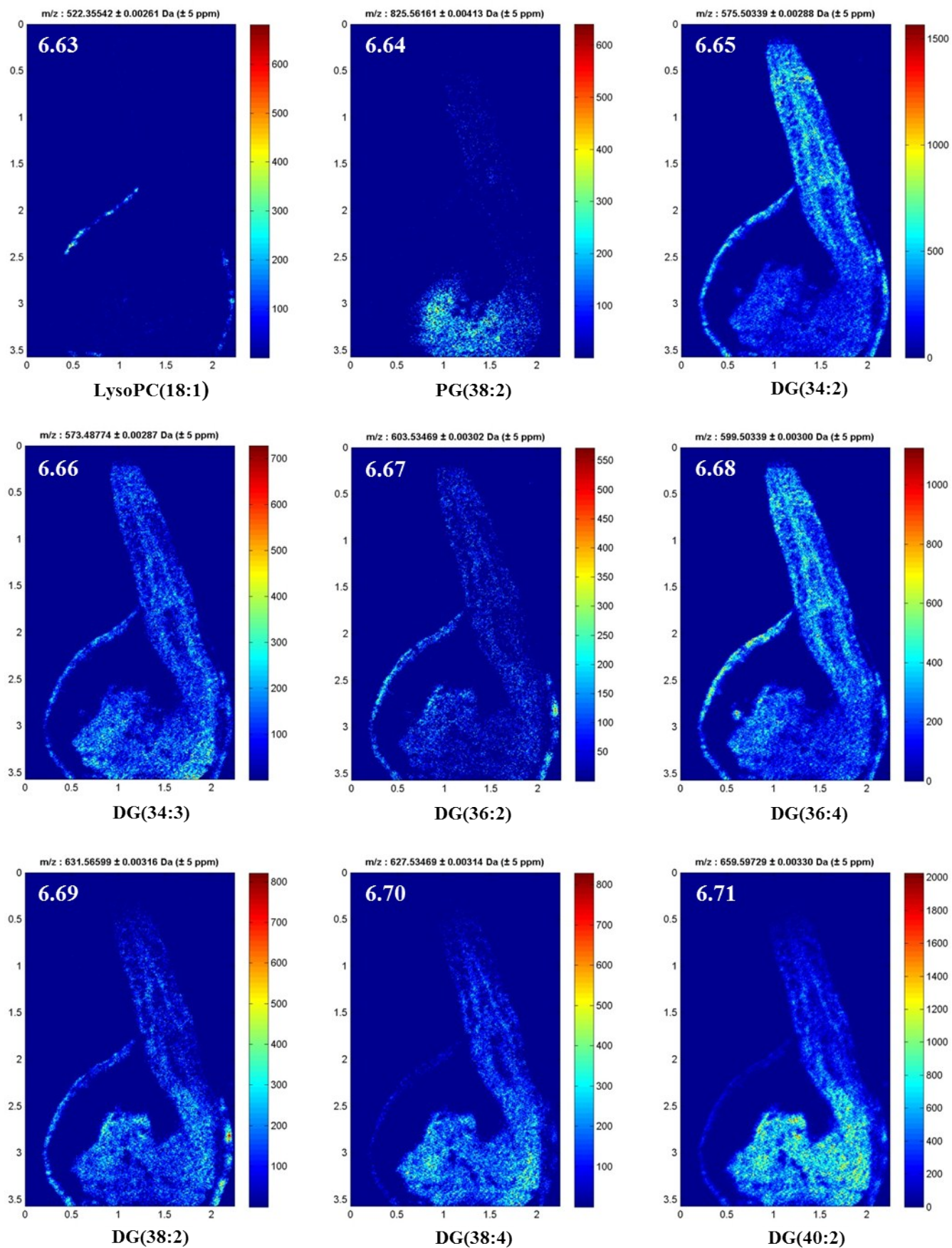


Fig. S6: continuation sheet

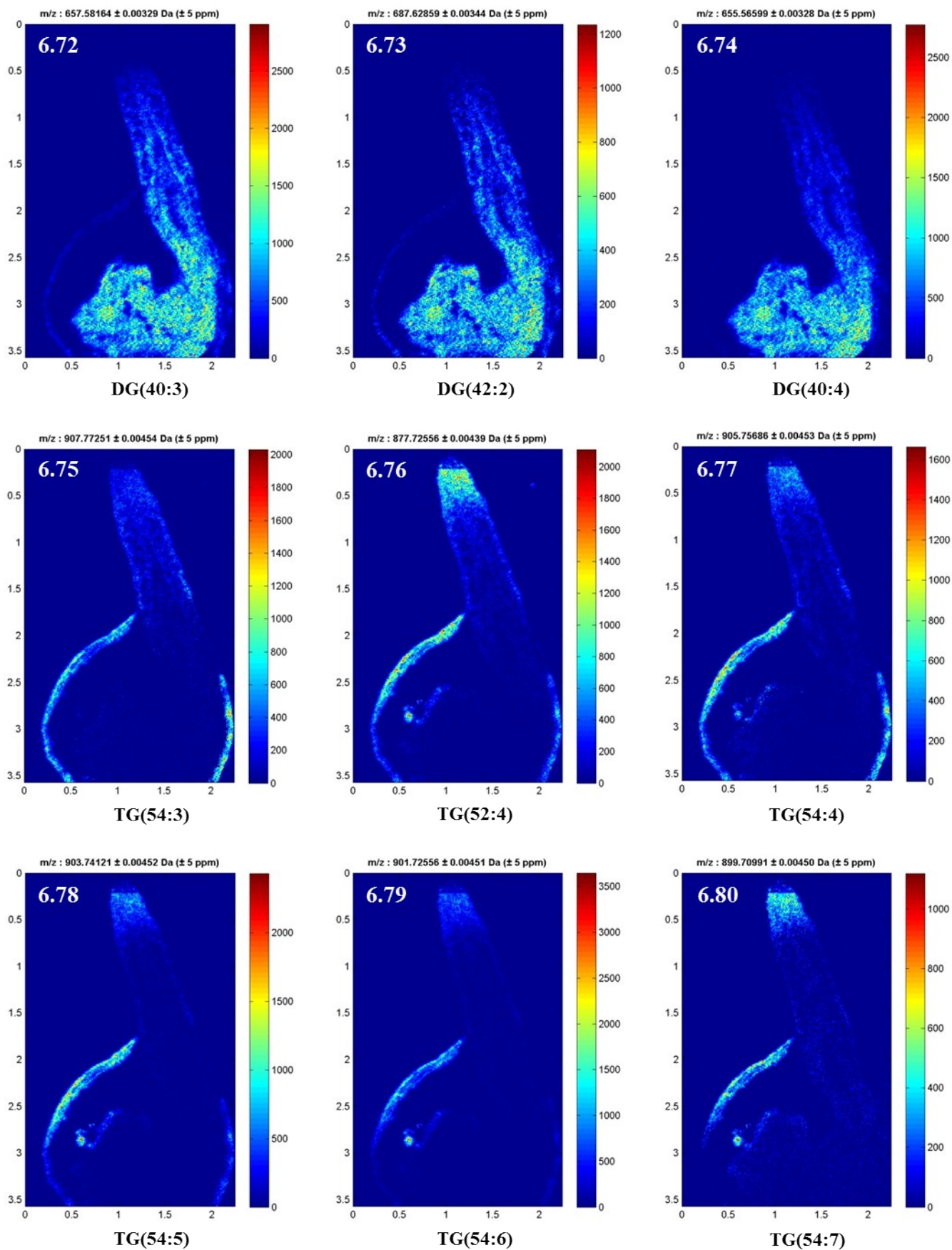


Fig. S6: continuation sheet

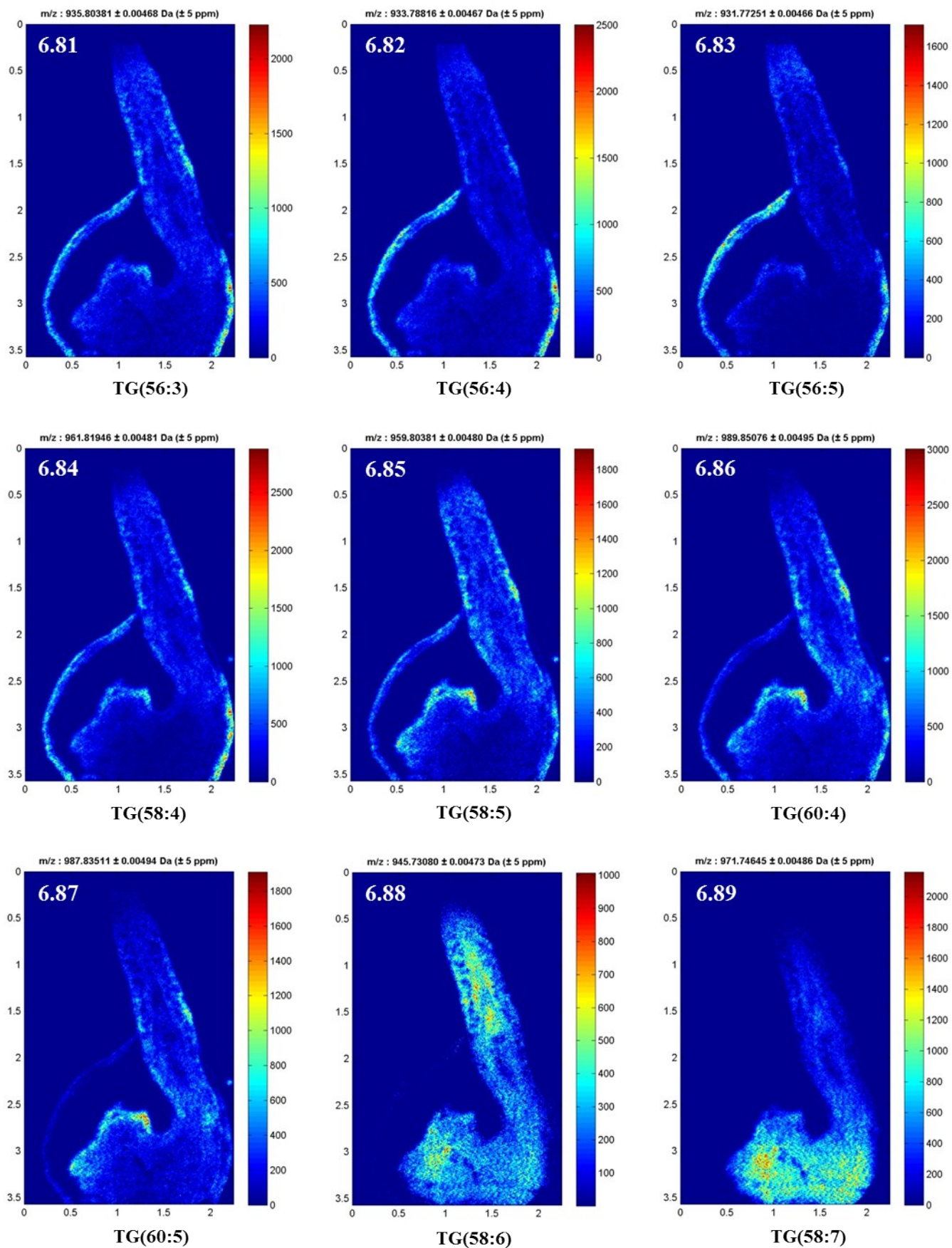


Fig. S6: continuation sheet

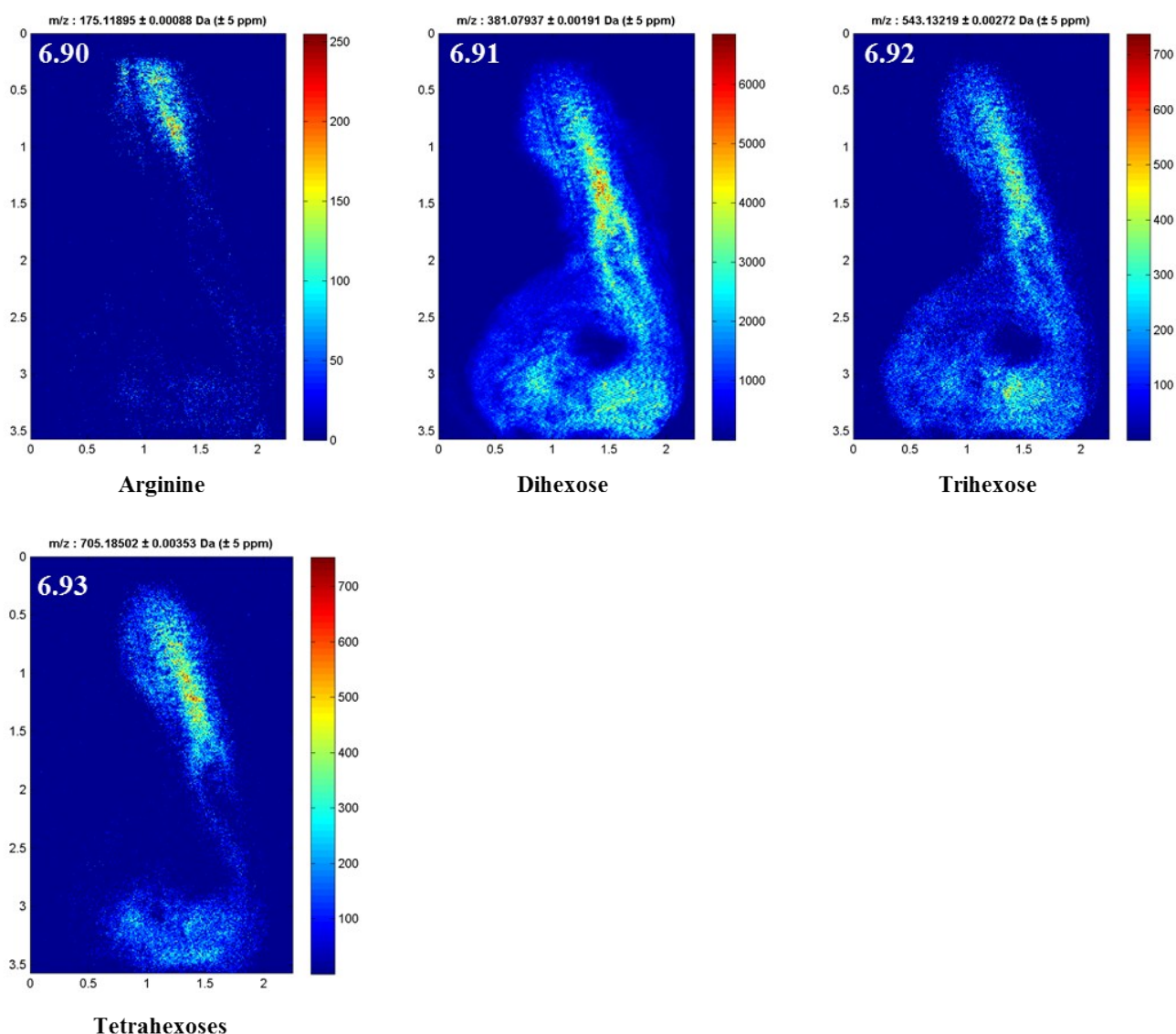


Fig. S6. Selected ion images of metabolites detected in germinating oilseed rape. Fig. S6.0 shows the optical image of a seed at the early germination stage. The longitudinal section of 20 μm thickness was obtained by 4.0% CMC embedding and cyrosectioning. The anatomy of early germinating seed comprises root tip (RT) which contains the root apical meristem (RAM) epidermis tissue (Ep), parenchyma tissue (Pa), vascular tissue (Va), shoot apical meristem (SAM), seed coat (S), endosperm (E), putative nucellar tissue (NT), abEp (abaxial epidermis), adEp (adaxial epidermis), outer and inner cotyledone (OC and IC); hypocotyl (H); radicle (R). Scale bar, 500 μm . MS images were generated with 225 x 357 pixels in positive ion mode, 10 μm step size; bin width: $\pm 5\text{ppm}$.

Fig. S7 Selected ion images of metabolites detected in mature oilseed rape

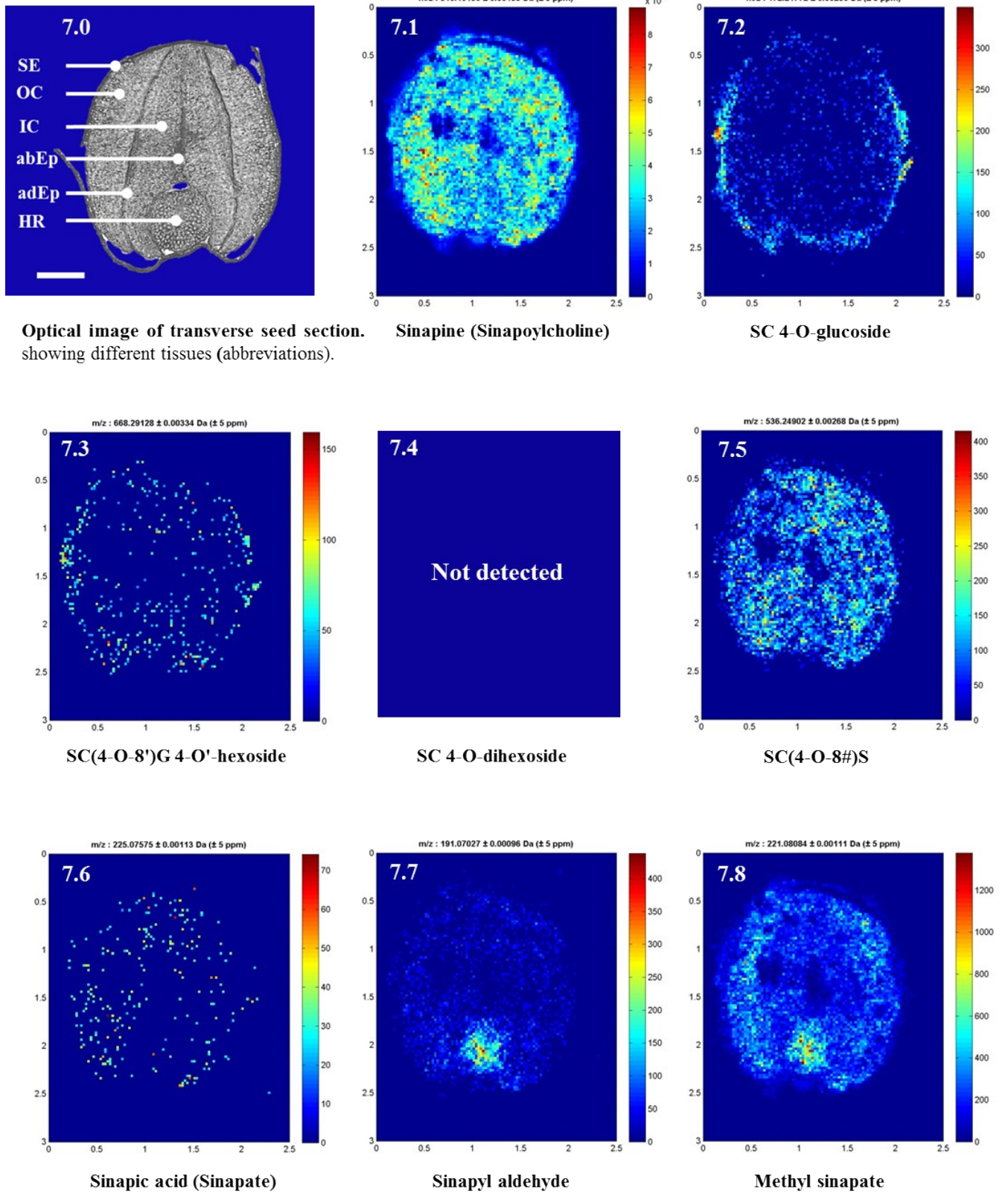


Fig. S7: continuation sheet

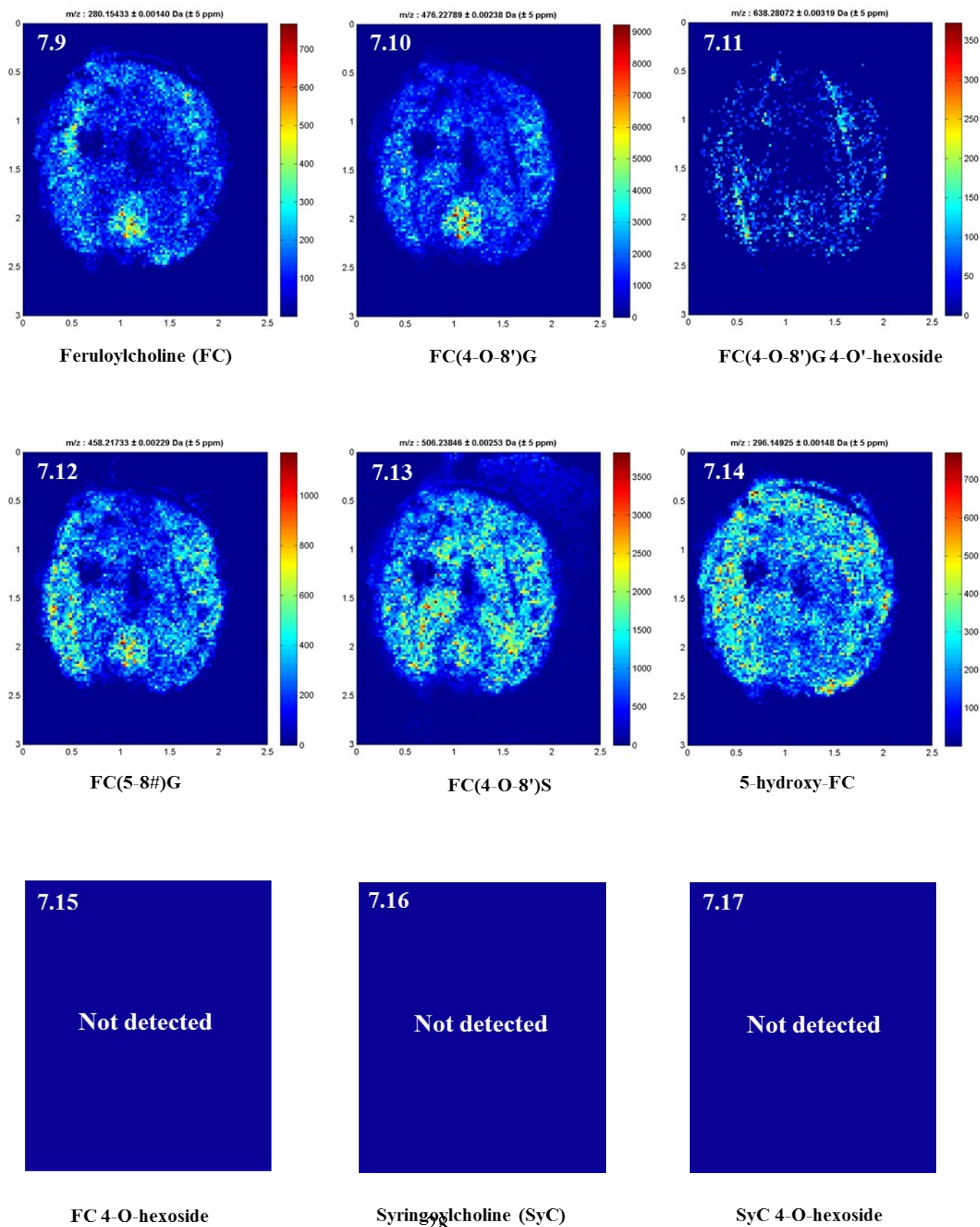


Fig. S7: continuation sheet

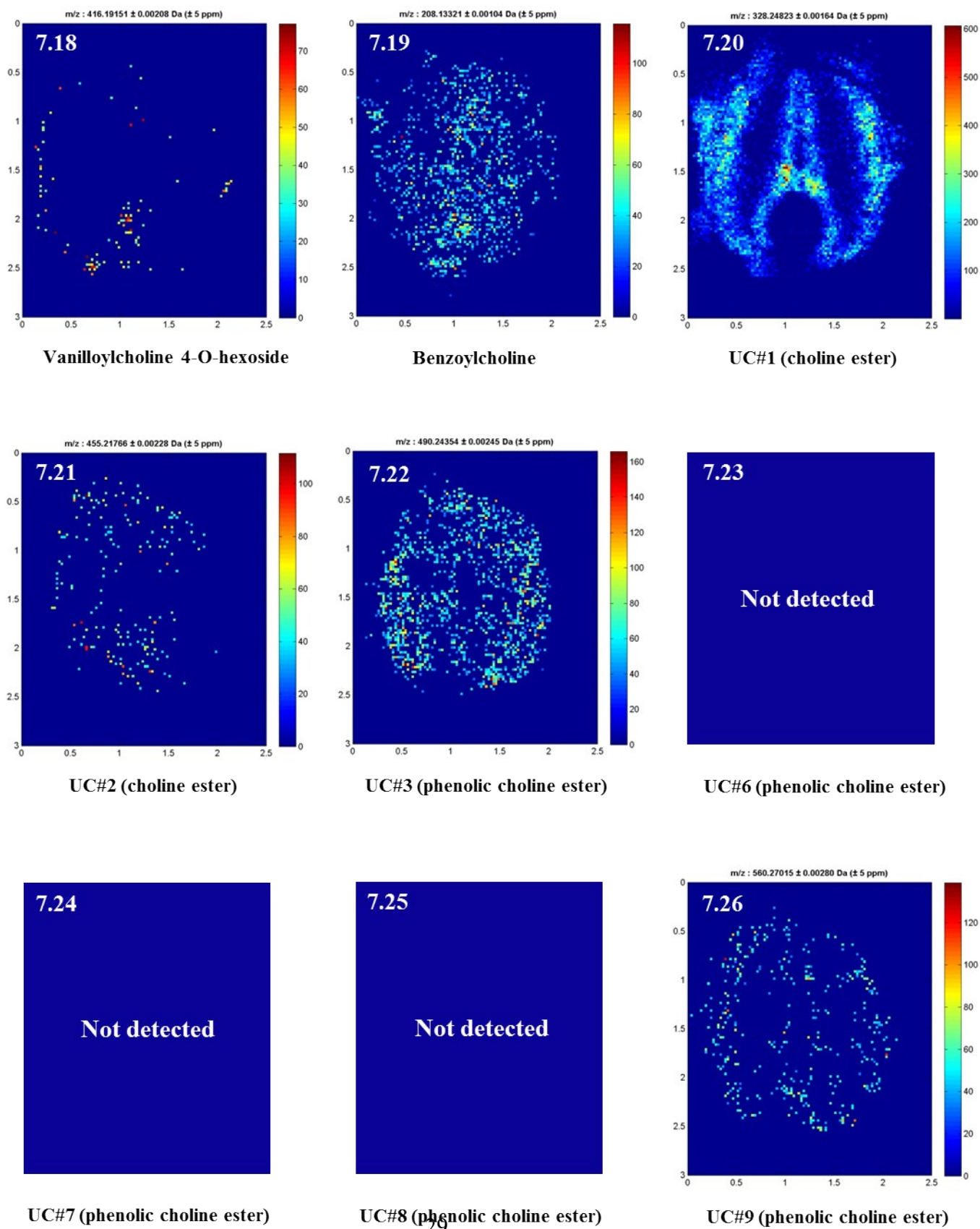


Fig. S7: continuation sheet

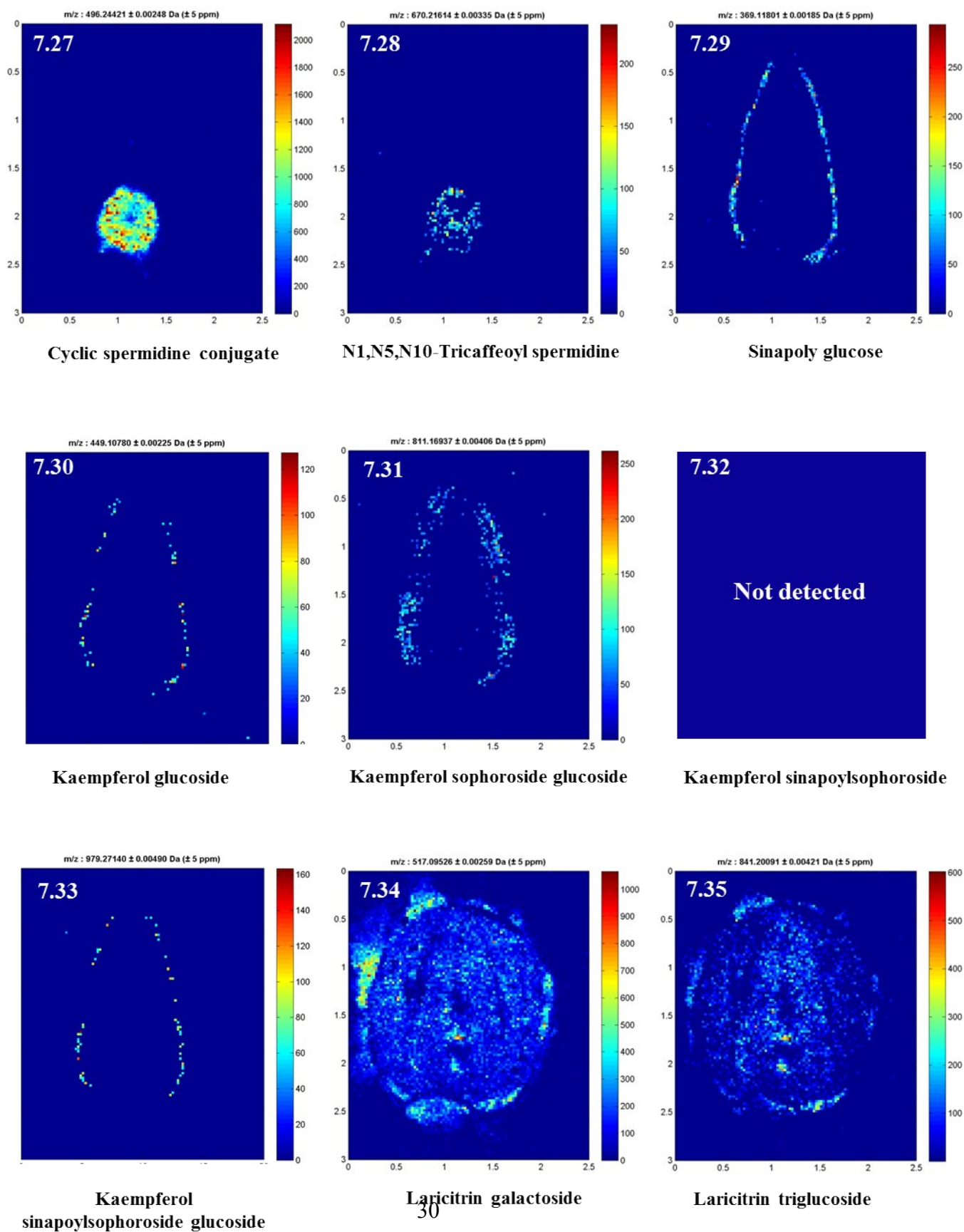


Fig. S7: continuation sheet

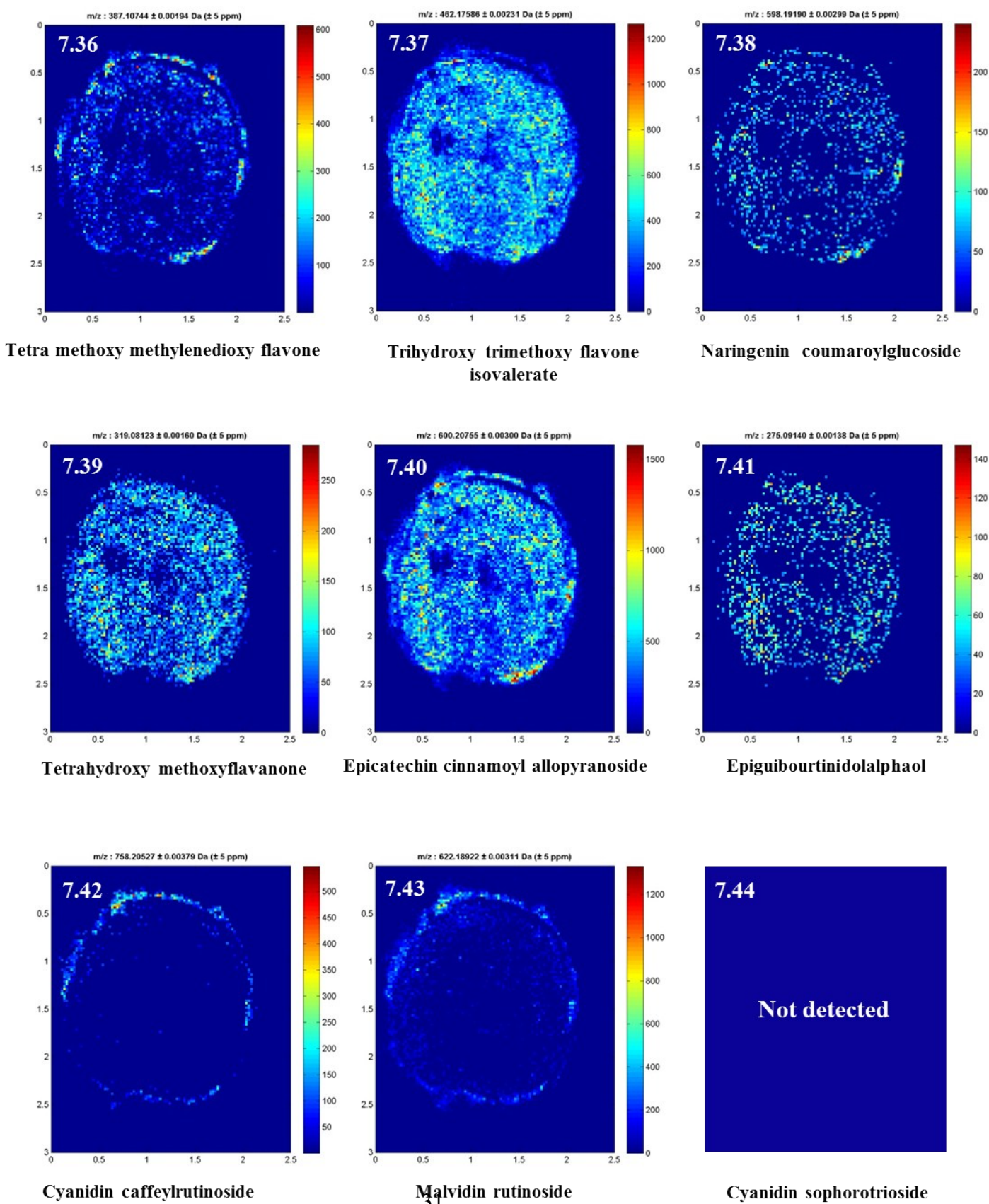


Fig. S7: continuation sheet

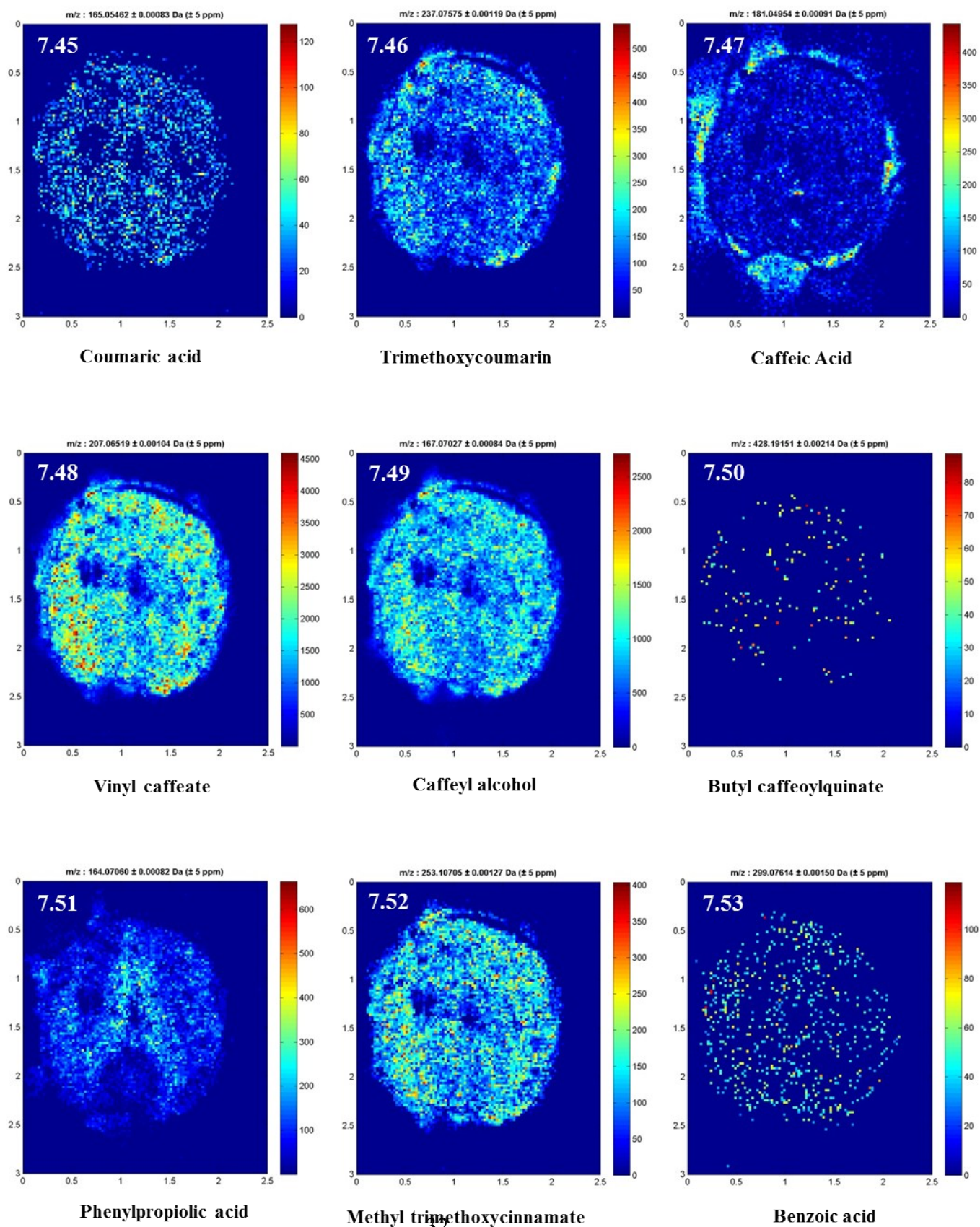


Fig. S7: continuation sheet

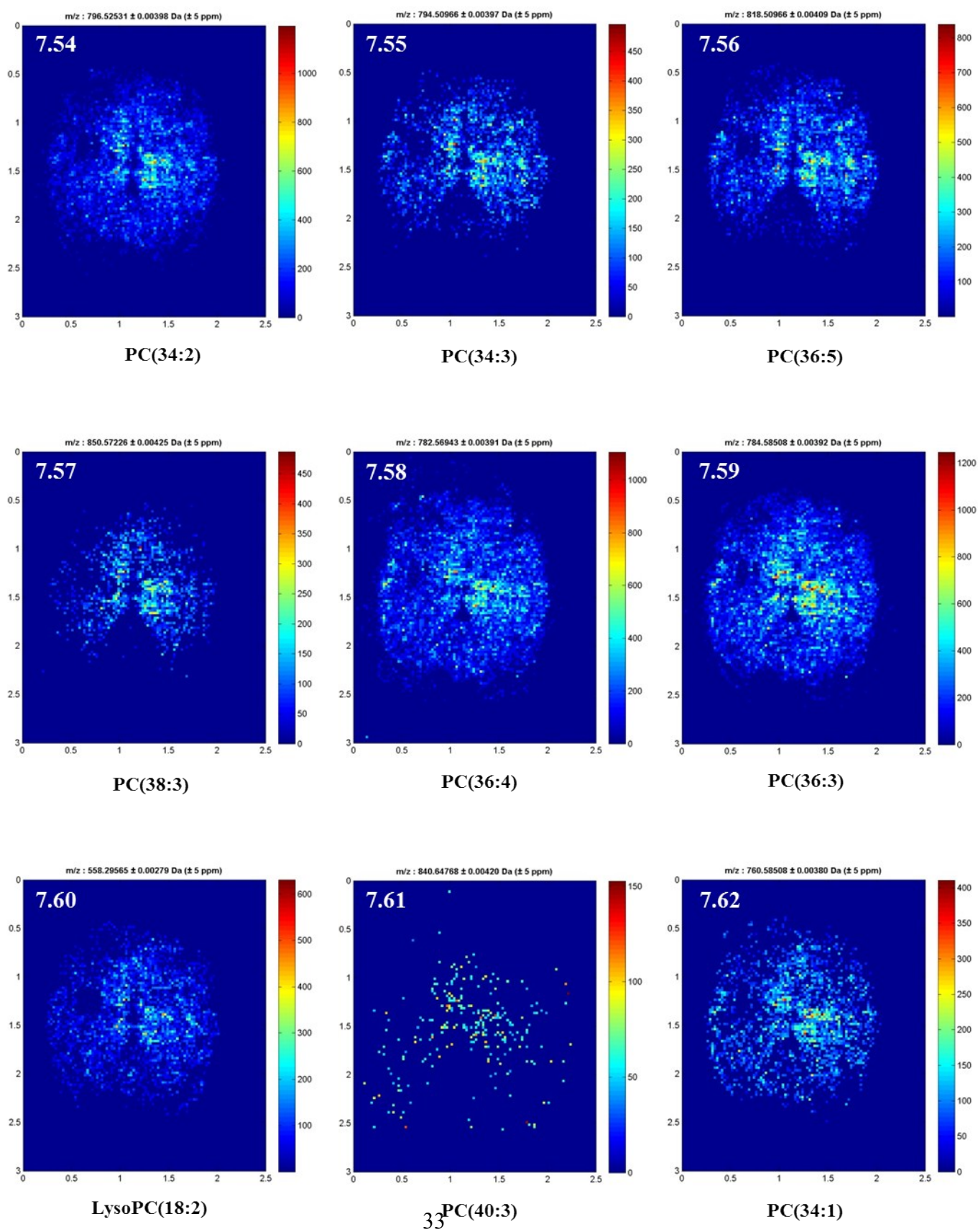


Fig. S7: continuation sheet

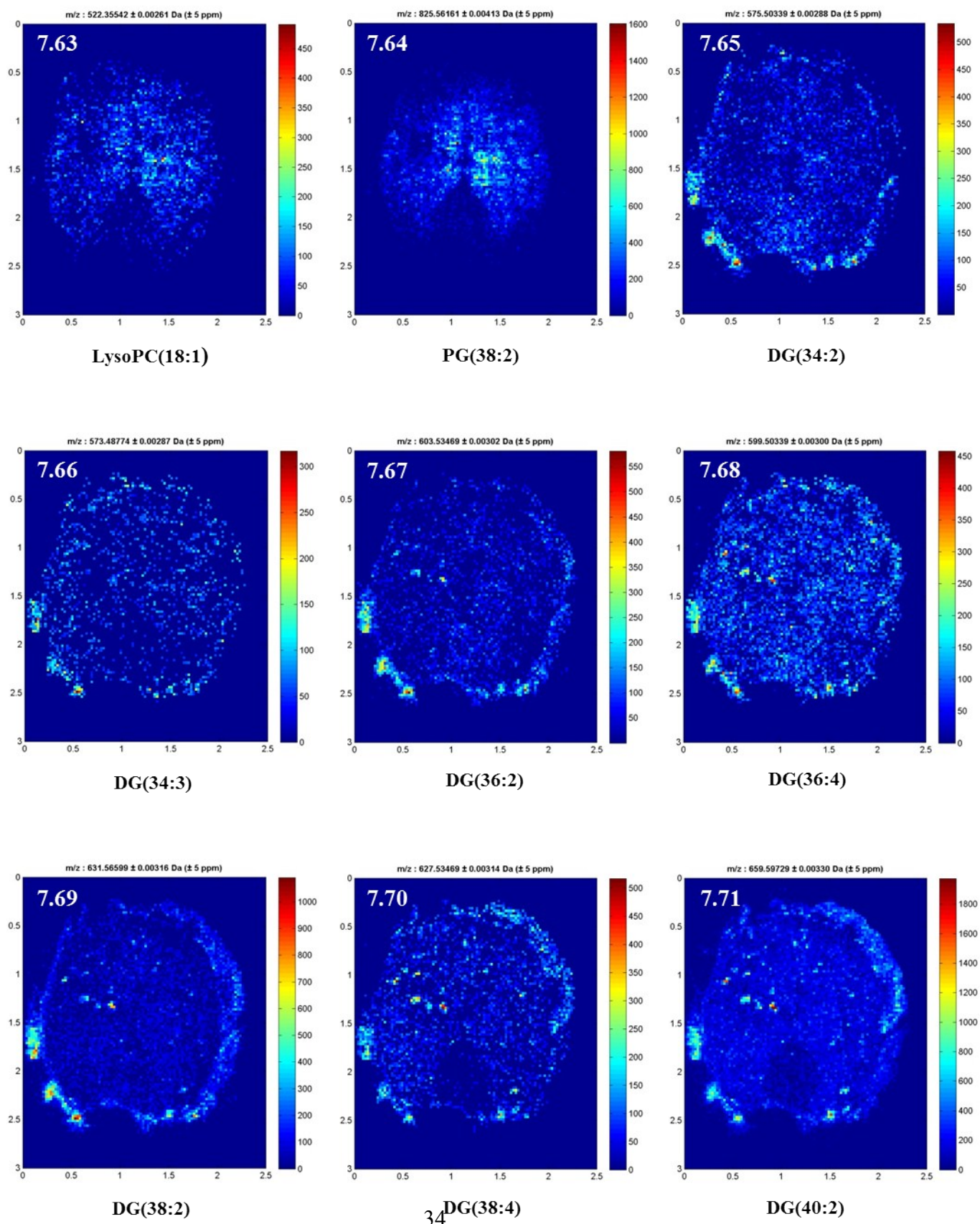


Fig. S7: continuation sheet

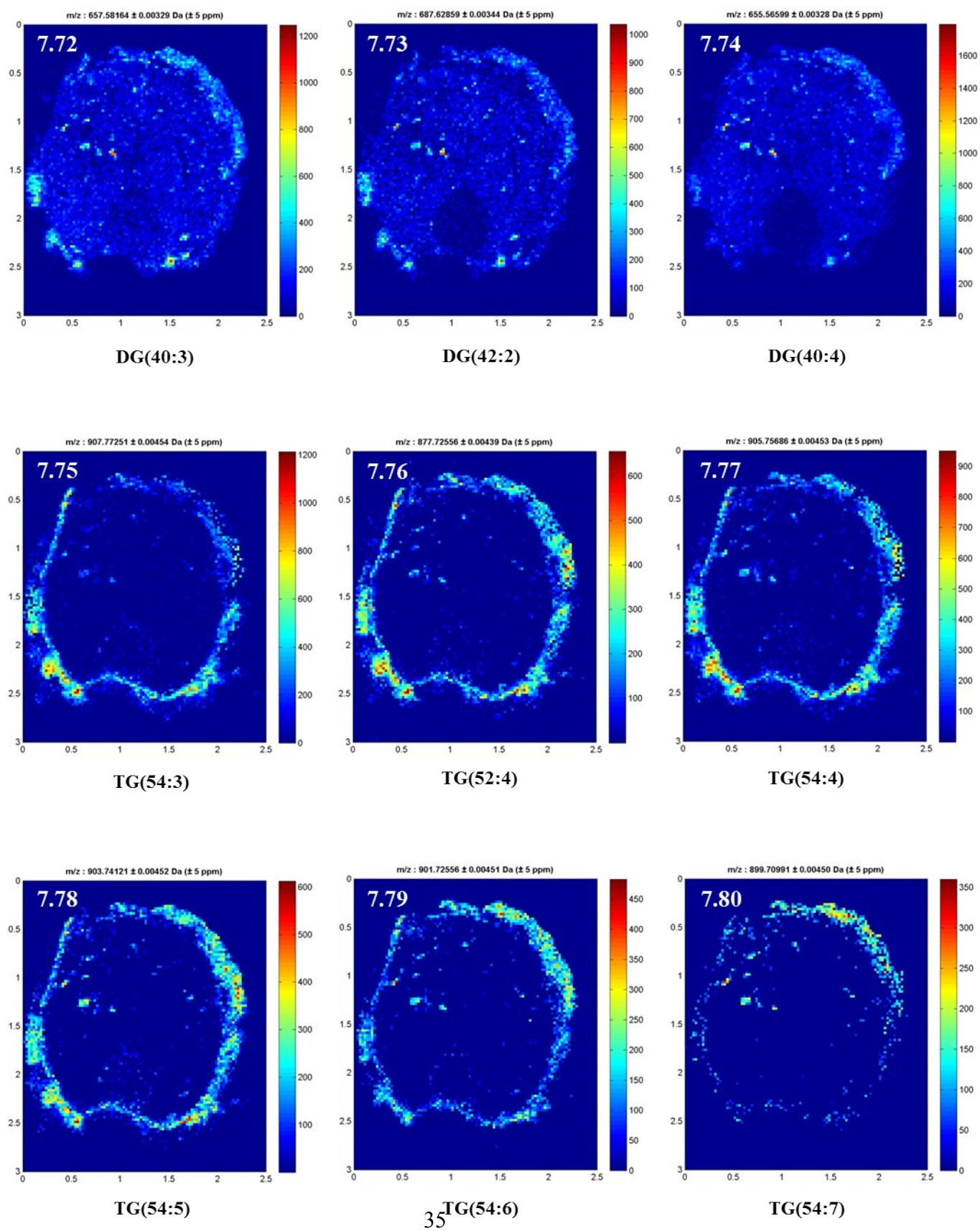


Fig. S7: continuation sheet

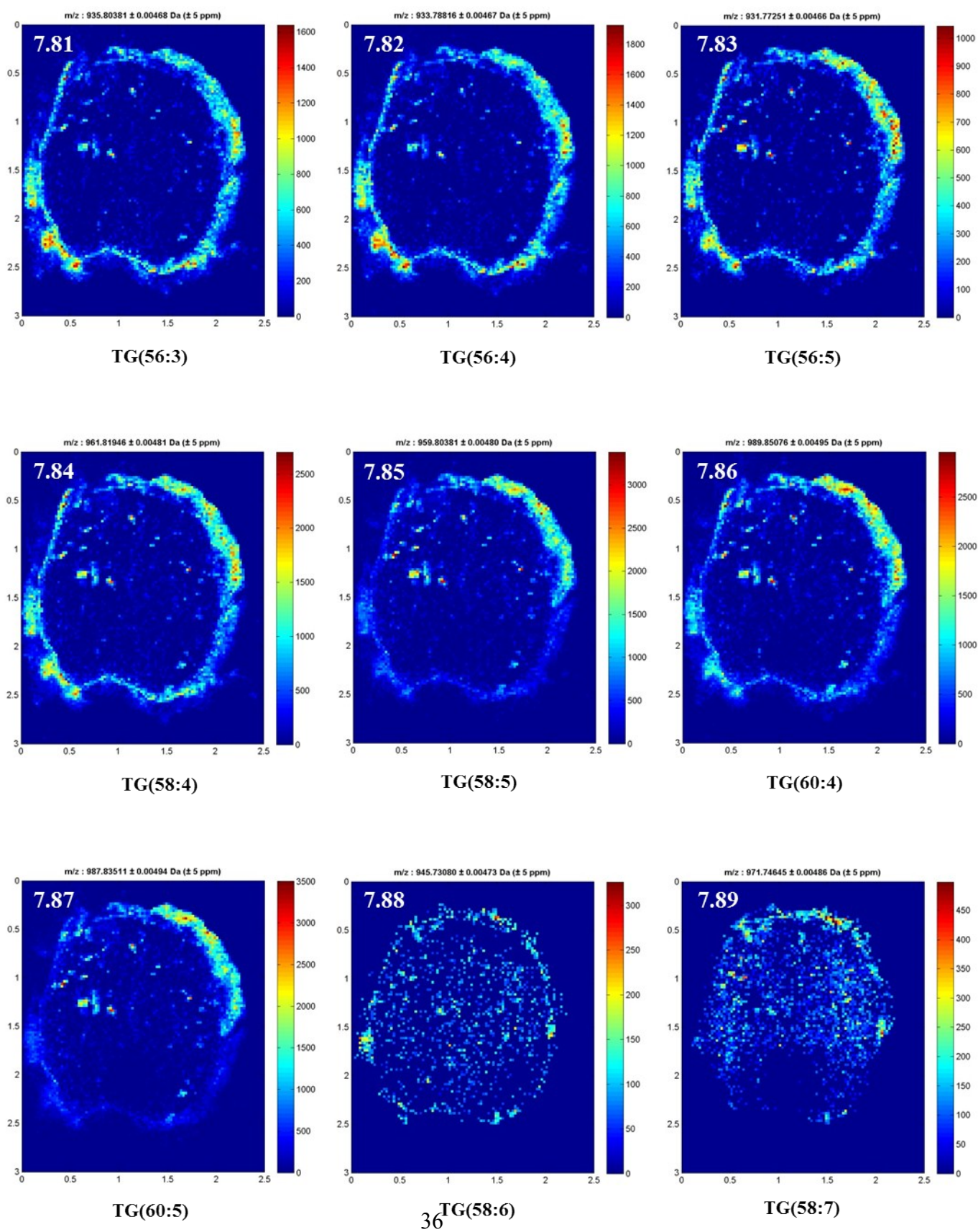


Fig. S7: continuation sheet

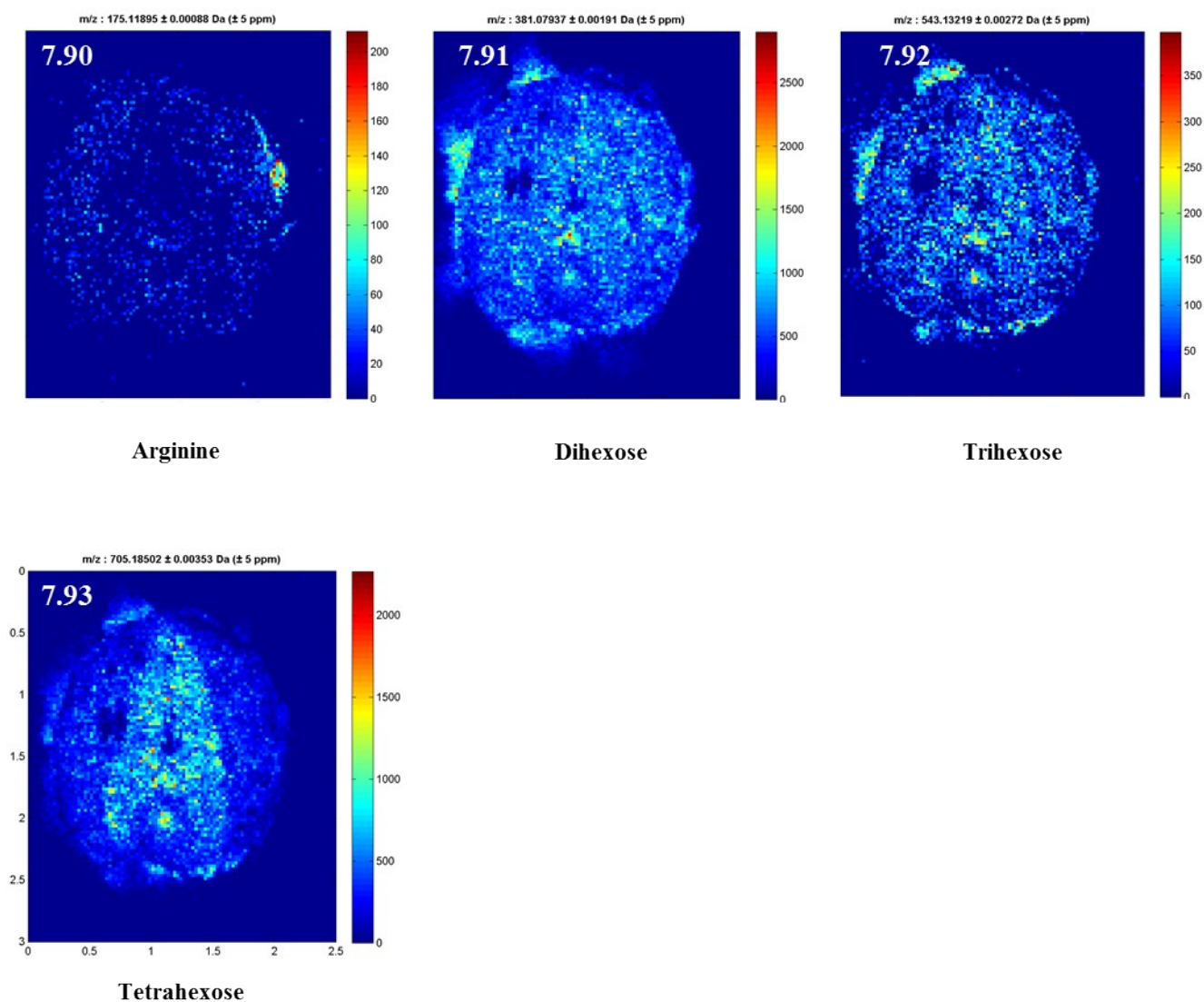


Fig. S7. Selected ion images of metabolites detected in mature oilseed rape. Fig. S7.0 shows the optical image of a seed at the maturation stage. The cross section of 20 μm thickness was obtained by 4.0% CMC embedding and cyrosectionining. The anatomy of mature seed comprises the embryo structures hypocotyl-radicle region (HR); abEp (abaxial epidermis), adEp (adaxial epidermis); outer and inner cotyledone (OC & IC); cuticula of cotyledons (Cu); and the seed coat-endosperm region (SE). Scale bar, 500 μm . MS images were generated with 100 x 120 pixels in positive ion mode, 25 μm step size; bin width: \pm 5ppm.

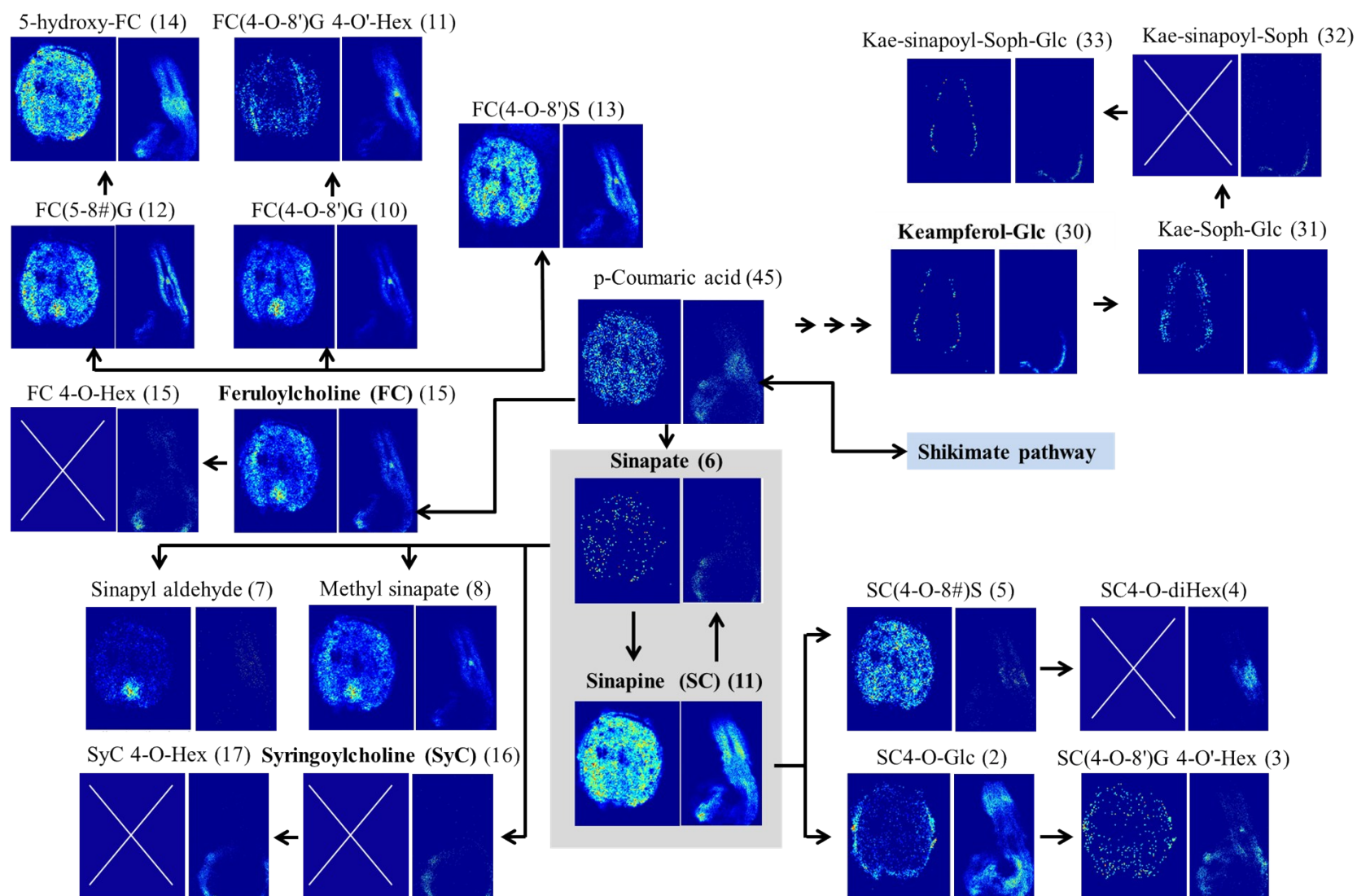


Fig. S8. Scheme of metabolomic network associated with sinapate ester metabolism, localized by high-resolution MS imaging in mature and early germinating oilseed rape. (Identical to Figure 2 in main text).

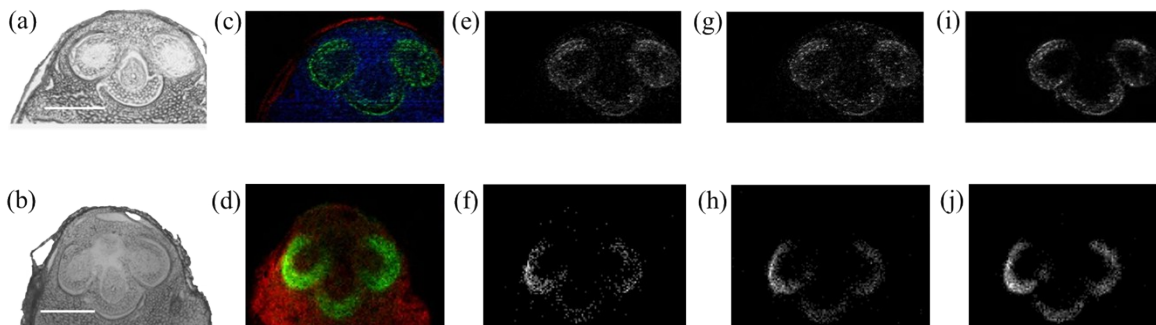


Fig. S10. MS imaging of wheat seed in positive and negative ion mode. (a) and (b) Optical images of 20 μm cross sections prepared from the wheat germ at dough stage. The shown anatomy of germs is explained in Fig. 3 and 4, respectively. Scale bars 500 μm . (c) Overlay of three ion images generated in positive ion mode, showing the spatial distributions of a polyphenol glycoside $[\text{M}+\text{K}]^+$, m/z 603.11107 (green), located in the protection sheath coleoptile/coleorhizae; and of a phosphatidylcholine $[\text{PC}(36:4)+\text{K}]^+$, m/z 820.52531 (blue) in the scutellum (monocot cotyledon); as well as the location of a phosphatidylglycerol $[\text{PG}(38:2)+\text{H}-\text{H}_2\text{O}]^+$, 785.56910 (red), specific for the pericarp-seed coat. MS images were generated with 320 x 180 pixels, 5 μm pixel size, and a m/z bin width of $\Delta m/z \pm 5$ ppm. (d) Overlay of two ion images, generated in negative ion mode showing a phosphatidylinositol $[\text{PI}(34:2)-\text{H}]^-$, m/z 833.51855 (red), located in the coleoptile/coleorhizae; and a polyphenol glycoside $[\text{M}-\text{H}]^-$, m/z 563.14063 (green) distributed in the scutellum. MS images were generated with 150 x 150 pixels, 15 μm pixel size, and a m/z bin width of $\Delta m/z \pm 5$ ppm. (e) - (j) Direct comparisons between positive and negative ion mode measurements. (e), (g) and (i) show polyphenol glycosides detected at positive ion mode $[\text{M}+\text{H}]^+$ with m/z 535.14462, 547.14462 and 771.21309 respectively; (f), (h) and (j) show the same polyphenol glycosides detected at negative ion mode with m/z 533.13006 $[\text{M}-\text{H}]^-$, 545.13006 $[\text{M}-\text{H}]^-$ and 769.19854 $[\text{M}-\text{H}]^-$, respectively.

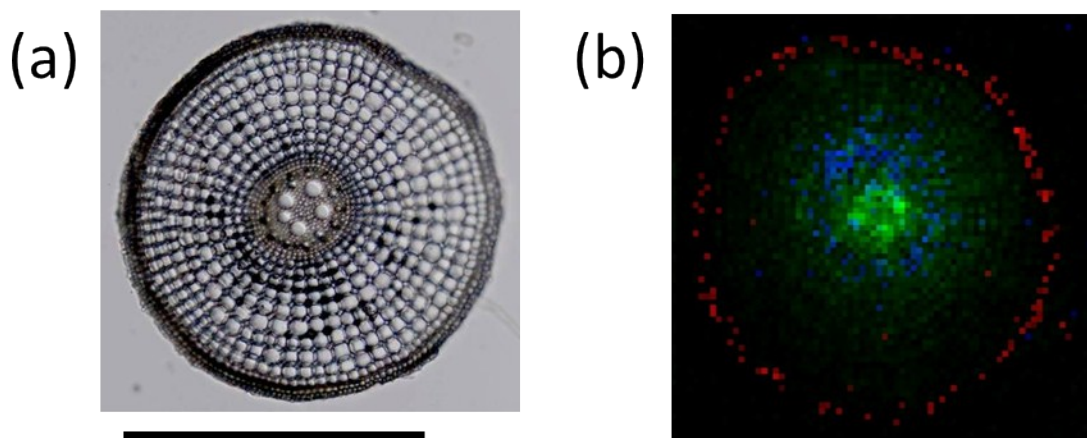


Fig. S11. MS imaging of rice root cross section taken from the elongation zone. (a) Optical image of adventitious rice root. The shown anatomy of root section is explained in Fig. 7, with the exception of root hairs which are not developed at this root zone located directly behind the apical meristem and root cap (protection sheath). (b) Overlay of three ion images generated with polyphenol glycoside $[M+H]^+$, m/z 803.22405 (red) located exclusively in the rhizodermal layer; the lysophosphatidylcholine $[lysoPC(16:0)+K]^+$, m/z 534.29565 (green) which is evenly distributed in the central root column (stele) containing the vascular bundles; and the phosphatidylcholine $[PC(36:4)+K]^+$, m/z 782.56943 (blue) located in the central cortex region. MS images were generated with 75 x 75 pixels; 10 μm pixel size; m/z bin width: $\Delta m/z \pm 5$ ppm. Scale bar 500 μm .

Experimental details: Sections from the root elongation zone were prepared manually using a common shaving blade. Thereby, the root was held in between a Styrofoam[®]. Then the blade was moved from top to bottom, tangential to the Styrofoam[®] to obtain thin root sections. Afterwards the obtained section was placed on a glass slide before matrix application. The MS imaging experiment covered an area of 750 x 750 μm^2 (75 x 75 pixels) with 10 μm step size. Mass spectra were obtained with the range of m/z 100-1000 and the mass spectrometer was set to a mass resolution of 100,000 @ m/z 200.

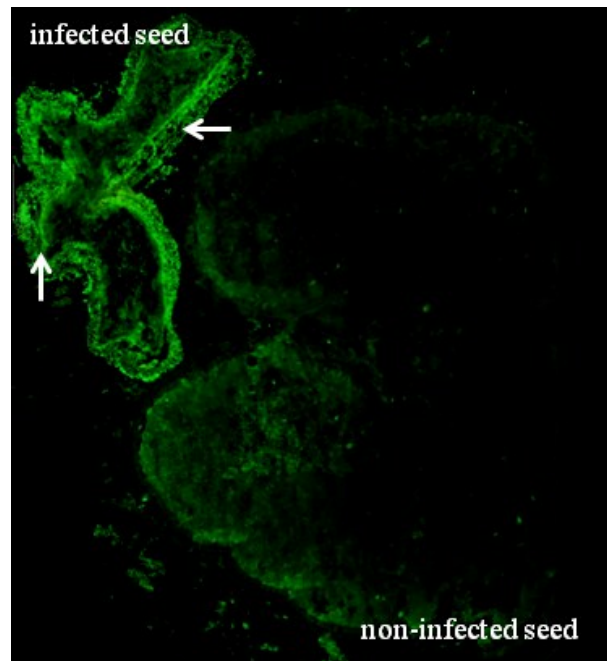
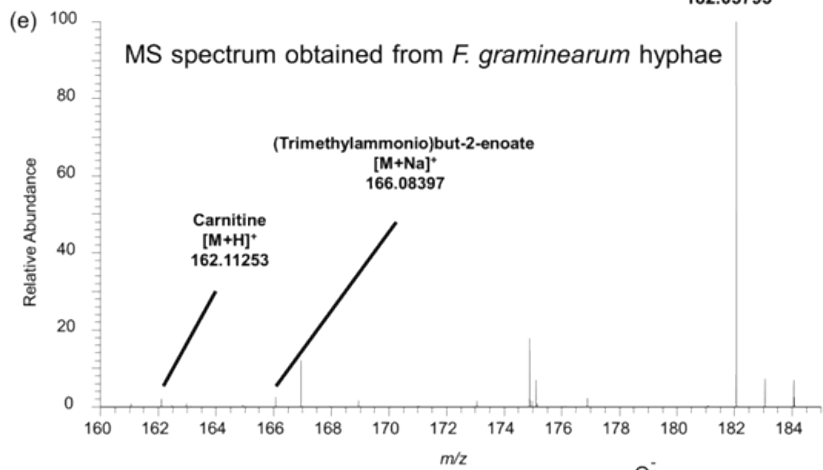
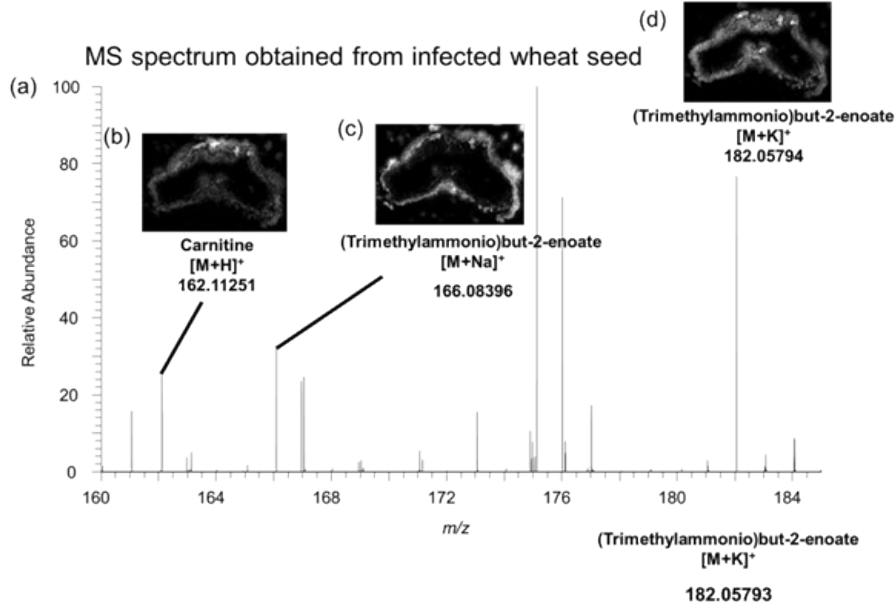


Fig. S12. Fluorescence microscopy on cross sections of *Fusarium graminearum* infected and uninfected wheat seed. The microscopic images of infected (left) and healthy (right) wheat seeds demonstrate the characteristic weight reduction, shrivelled and light-brown appearance of infected seeds. The cross section of infected seed shows green stained fungal hyphae specifically located in the entire bran of seed, indicated by white arrows.

Experimental details: To visualize internal hyphae, seed tissues were stained by using a WGA (Wheat Germ Agglutinin) Alexa Fluor 488[®] conjugate (Invitrogen, Life technologies, Germany) solution in 1*PBS (pH 7.4) for 20 min at room temperature. Finally, tissues were washed twice by using doubly distilled water.



MALDI MS/MS spectrum of *m/z* 182.05779

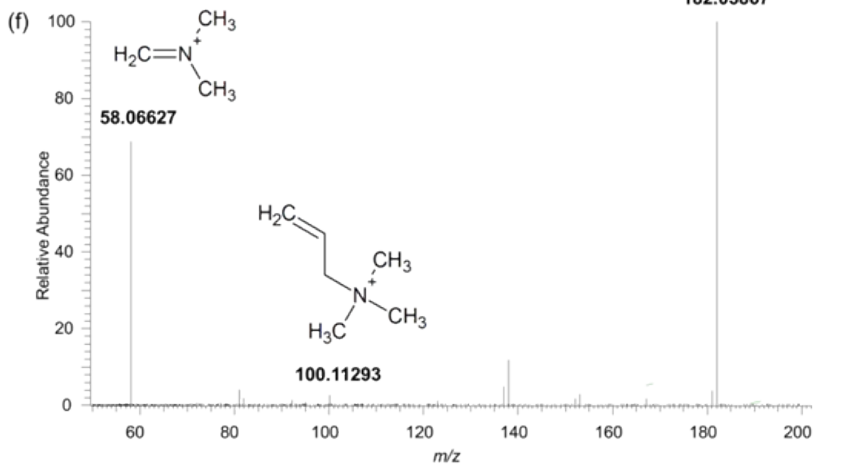


Fig. S13. Detection of carnitine and (trimethylammonio)but-2-enoate metabolites in wheat seed infected with *Fusarium graminearum*. This fungal pathogen is a major causal agent of the head blight disease in cereal crops. Signals of both metabolites were detected by MALDI-MS measurements on *F. graminearum* hyphae after matrix application and also by MS imaging on *F. graminearum* infected seed of the highly FHB susceptible spring wheat cultivar Florence-Aurore. (a) MS spectrum from the infected wheat seed at 15 μm pixel size. Compounds specifically mapped to the infected bran layer are (b) the carnitine $[\text{M}+\text{H}]^+$, m/z 162.11247; and two adducts of (trimethylammonio)but-2-enoate (c) $[\text{M}+\text{Na}]^+$, m/z 166.08385 and (d) $[\text{M}+\text{K}]^+$, m/z 182.05779. All shown MS images were generated with 155 x 105 pixels; 15 μm pixel size; m/z bin width: $\Delta m/z \pm 5\text{ppm}$. Optical and MS images on infected seed are also shown in Fig. 8. (e) MALDI MS spectrum obtained from *F. graminearum* hyphae. (f) MS/MS spectrum of (Trimethylammonio)but-2-enoate $[\text{M}+\text{K}]^+$, m/z 182.05779.

Experimental details: *F. graminearum* hyphae of isolate 'IFA 65' (IFA Tulln, Austria) were cultivated on Synthetic Nutrient Deficient Agar (SNA)' (Nirenberg, 1976) at 20 °C under cool-white and near-UV light illumination. After 10 days fungal hyphae were taken by a scapula and kept on a glass slide. Before profiling the fungus by MALDI-MS, a DHB matrix was applied to *Fusarium* hyphae.

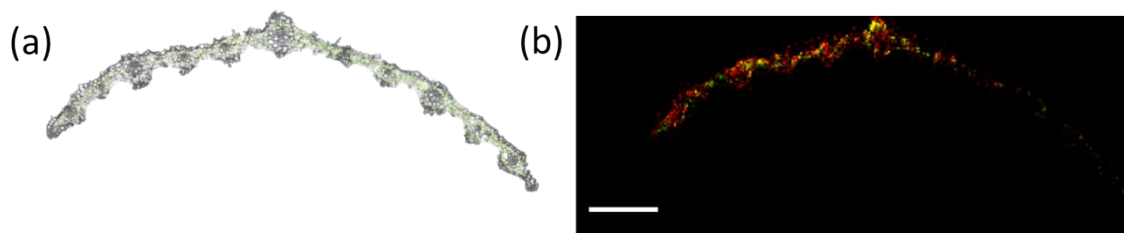


Fig. S14. MS imaging of wheat leaf blade. (a) Optical image of 20 μm cross section prepared from a lower leaf blade harvested at the first stem node. (b) Overlay of three ion images showing a phosphatidylcholine $[\text{PC}(34:3)+\text{K}]^+$, m/z 794.50966 (red); and pheophytin a $[\text{M}+\text{K}]^+$, m/z 909.52908 (green). Scale bar, 500 μm . MS images were generated with 320 x 128 pixels; 10 μm pixel size; m/z bin width: $\Delta m/z \pm 5$ ppm. Both compounds represent each a lipid and pigment with relevant, but different functional roles during leaf senescence and wilting processes in consequence of biological aging or stress. Thereby, the lipid PC behaves as an intermediate in betaine biosynthesis. As demonstrated in wheat and barley leaves betaine is a metabolic end product accumulated by wilted leaves (Ref.). Generally, PC is significantly accumulated in stressed leaves, possibly as part of an adaptive response. The pigment pheophytin a is a product of the chlorophyll a degradation during leaf desiccation. Pheophytin is stable and remains for long periods in dry leaves and soil organic matter layers (Ref.). Therefore, the detection of this pigment is an indication for the fast chlorophyll degradation in consequence of tissue sampling. Experimental details: Wheat leaf sections were obtained from 21 days old plants (begin of tillering, Z21-22). The leaf blade was snap frozen in 4% (w/v) carboxymethylcellulose (CMC) solution. A coolant mixer (hexane and dry ice) was use for snap freezing. Afterwards the obtained CMC block was transferred to the cryostat for sectioning. The MS imaging experiment covered an area of 3200 x 1280 μm^2 (320 x 128 pixels). Mass spectra were acquired in positive ion mode in the mass range m/z 400 –1000. The mass resolution of the instrument was set to 70,000@ m/z 200.

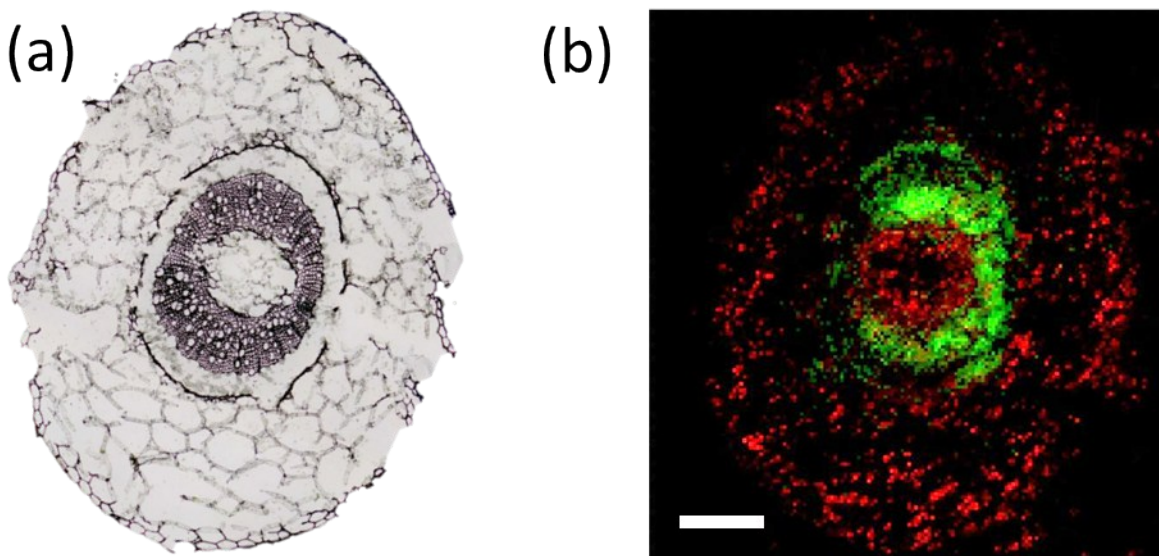


Fig. S15. MS imaging of young oilseed rape stem. (a) Optical image of 20 μm stem cross section harvested from a three weeks old oilseed rape plant. The section taken from midst of the young stem was obtained after embedding in 4% CMC. (b) Overlay of two ion images generated with the pheophytin a $[\text{M}+\text{K}]^+$, m/z 909.52908 (red) detected in the cortex and central pith; and the phosphatidylcholine $[\text{lysoPC}(16:0)+\text{K}]^+$, m/z 534.29565 (green) specifically present in the cylinder with vascular vessels which is located between pith and cortex. MS images 155 x 164 pixels; 20 μm pixel size; m/z bin width: $\Delta m/z \pm 5$ ppm. Scale bar 500 μm .

Experimental: Oilseed rape stem sections were obtained from 21 days old plants (begin of tillering, Z21-22). The stem was embedded in 4% (w/v) carboxymethylcellulose (CMC) solution first at 20 $^{\circ}\text{C}$ for 20 minutes, followed by 30 minutes at -80 $^{\circ}\text{C}$. Then the CMC block was transferred to the cryomicrotome to produce the sections. The MS imaging experiment covered an area of 3100 x 3280 μm^2 (155 x 164 pixels). Mass spectra were acquired in positive ion mode in the mass range m/z 100 –1000. The mass resolution of the instrument was set at 50,000@ m/z 200.

Methods S1. Chemicals

Matrixes; 2,5-dihydroxybenzoic acid (DHB); 4-nitroaniline; and hexane were purchased from Fluka Sigma-Aldrich (Sweden). Glass microscope slides (ground edges frosted) were obtained from VWR International (Darmstadt, Germany). Carboxymethyl cellulose (CMC), sodium salt was purchased from Sigma Life Science (Missouri, USA) and tragacanth from Sigma-Aldrich (Steinheim, Germany). All chemicals used in this study were of the highest available purity.

Methods S2. Generation of plant material

Oilseed rape (*Brassica napus* L.): Mature (Z00) and germinating (Z05) seeds ¹ used for the MS imaging approach were obtained from a back cross (BC₁F₂) line which originated from a cross between the two Chinese semi-winter oilseed rape lines ‘GH06’ and ‘P174’ ². For MS imaging on early germinating oilseed rape, seeds were initially double surface sterilized by a sequential immersion in 70% ethanol for 2 min, and in 1% sodium hypochlorite containing 0.1% Tween-20 for 15 min under constant shaking. Subsequently seeds were washed twice with autoclaved tap water and sown in a petri dish on filter paper. The petri dish was filled with 10 mL of sterilized water, sealed with Parafilm and kept at 27 °C in darkness until the radicle emerged from seed.

For MS imaging on oilseed rape stem, plants of the above mentioned BC₁F₂ line were grown in the greenhouse for three weeks at 22 °C in a greenhouse with a light regime of 14 h per day. Stem samples were immediately frozen in liquid nitrogen and stored at -80 °C until analysis.

Wheat (*Triticum aestivum* L.): All wheat organs analysed by MS imaging were obtained from the France spring wheat cultivar ‘Florence-Aurore’. For the MS imaging on wheat seed and spike rachis, plants were cultivated in the greenhouse with a 16/8 h light regime and temperatures of 22/18 °C (day/night). The spikes were harvested at soft dough stage (Z85), approximately 21 days after flowering. Seeds and spike rachis were each sampled from the centre of spike and immediately frozen in liquid nitrogen.

For MS imaging on wheat stem base and leaf blade, seeds were sterilized in 6% sodium hypochlorite for 40 minutes on a magnetic stirrer and were washed 10 times with distilled water. Seeds were sown in a 1:2 (v/v) mixture of autoclaved sand and soil (Fruhstorfer Erde, Hawita Gruppe GmbH, Germany). The cultivation has been carried out in a climate chamber with a 16 h photoperiod of 22 °C/18 °C and 60% humidity for three weeks until begin of tillering stage

(Z20). The stem base and leaf blade tissues were excised and immediately frozen in liquid nitrogen.

For MS imaging on wheat seeds infected with *F. graminearum* wheat plants were grown in the greenhouse. After vernalisation at 4 °C for eight weeks with a 16/8 h day/night light regime, plants were cultivated at temperatures of 22/18°C with a photoperiod of 16/8 h (day/night). At early anthesis single floret inoculation with the *F. graminearum* strain 'IFA 65' was carried out by pipetting 10 µl of the fungal suspension (5×10^4 macroconidia mL⁻¹) between the palea and lemma of each floret. Control (mock) plants were inoculated with distilled water instead of the macroconidia suspension. Eight florets per spike were inoculated. Greenhouse day temperature was increased to 24 °C to ensure optimum infection conditions. At ripening stage (Z92) inoculated seeds were harvested and immediately frozen in liquid nitrogen³. All plant samples used for MS imaging were stored at -80 °C until analysis.

Rice (*Oryza sativa* L.): Seeds of the rice cultivar 'IR651' were kindly offered by Rice and Citrus Research Institute (RCRI), Agricultural Science and Natural Resources University, Sari, Iran. Rice seedlings were generated from sterilized seeds shown in petri dishes for 7 days in darkness at 27 °C. For MS imaging on *in vitro* grown roots, seeds were sterilized as described above and sown in petri dishes on filter paper. The petri dishes were filled with 10 mL of sterilized water, sealed with parafilm and kept at 27 °C in darkness for 7 days. Each six plant seedlings were then transferred to a glass bottle (10 cm diameter and 20 cm depth) containing 110 mL of N6 (+0.4% agar) growth cultivation media. Seedlings were cultivated in a phytotron at a thermoperiod of 27±0.5 °C; a photoperiod of 16 h; a relative humidity 60%; and a photon flux density of 220 µM/m²/S. After three weeks (begin of tillering stage, Z20) wheat roots were harvested and immediately frozen in liquid nitrogen.

Reference:

1. J. C. Zadoks, T. T. Chang and C. F. Konzak, *Weed Research*, 1974, **14**, 415-421.
2. L. Liu, A. Stein, B. Wittkop, P. Sarvari, J. Li, X. Yan, F. Dreyer, M. Frauen, W. Friedt and R. J. Snowdon, *TAG. Theoretical and applied genetics. Theoretische und angewandte Genetik*, 2012, **124**, 1573-1586.
3. S. Gottwald, B. Samans, S. Lück and W. Friedt, *BMC Genomics*, 2012, **13**, 1-22.